Ultrasensitive Chemical Analysis by Raman Spectroscopy

Katrin Kneipp,* Harald Kneipp, Irving Itzkan, Ramachandra R. Dasari, and Michael S. Feld

Physics Department, Technical University Berlin, D 10623 Berlin, Germany, and G. R. Harrison Spectroscopy Laboratory, Massachusetts Institute of Technology, Cambridge, Massachusetts 02139

Received February 17, 1999 (Revised Manuscript Received August 25, 1999)

Contents

1. Introduction

In the Raman effect, incident light is inelastically scattered from a sample and shifted in frequency by the energy of its characteristic molecular vibrations. Since its discovery in 1927, the effect has attracted attention from a basic research point of view as well as a powerful spectroscopic technique with many practical applications. The advent of laser light sources with monochromatic photons at high flux densities was a milestone in the history of Raman spectroscopy and resulted in dramatically improved scattering signals (for a general overview of modern Raman spectroscopy, see refs 1−5).

In addition to this so-called spontaneous or incoherent Raman scattering, the development of lasers also opened the field of stimulated or coherent Raman spectroscopies, in which molecular vibrations are coherently excited. Whereas the intensity of spontaneous Raman scattering depends linearly on the number of probed molecules, the coherent Raman signal is proportional to the square of this number (for an overview, see refs 6 and 7). Coherent Raman techniques can provide interesting new opportunities such as vibrational imaging of biological samples,[8] but they have not yet advanced the field of ultrasensitive trace detection. Therefore, in the following article, we shall focus on the spontaneous Raman effect, in the following simply called Raman scattering.

Today, laser photons over a wide range of frequencies from the near-ultraviolet to the near-infrared region are used in Raman scattering studies, allowing selection of optimum excitation conditions for each sample. By choosing wavelengths which excite appropriate electronic transitions, resonance Raman studies of selected components of a sample or parts of a molecule can be performed.[9]

In the past few years, the range of excitation wavelengths has been extended to the near-infrared (NIR) region, in which background fluorescence is reduced and photoinduced degradation from the sample is diminished. High-intensity NIR diode lasers are easily available, making this region attractive for compact, low cost Raman instrumentation. Further, the development of low noise, high quantum efficiency multichannel detectors (charge-coupled device (CCD) arrays), combined with high-throughput single-stage spectrographs used in combination with holographic laser rejection filters, has led to high-sensitivity Raman spectrometers (for an overview on state-of-the-art NIR Raman systems, see ref 10). As we shall show in section 2, the near-infrared region also has special importance for ultrasensitive Raman spectroscopy at the single-molecule level.

As with optical spectroscopy, the Raman effect can be applied noninvasively under ambient conditions in almost every environment. Measuring a Raman spectrum does not require special sample preparation techniques, in contrast with infrared absorption spectroscopy. Optical fiber probes for bringing excitation laser light to the sample and transporting scattered light to the spectrograph enable remote detection of Raman signals. Furthermore, the spatial and temporal resolution of Raman scattering are determined by the spot size and pulse length, respectively, of the excitation laser. By using a confocal microscope, Raman signals from femtoliter volumes ($\sim 1\ \mu m^3$) can by observed, enabling spatially resolved measurements in chromosomes and cells.[11] Techniques such as multichannel Hadamard transform Raman microscopy[12,13] or confocal scanning Fourier transform Raman microscopy[14] allow generation of high-resolution Raman images of a sample. Recently, Raman spectroscopy was performed using near-field optical microscopy.[15−17] Such techniques overcome the diffraction limit and allow volumes significantly smaller than the cube of the wavelength to be investigated. In the time domain, Raman spectra can be measured on the picosecond time scale, providing information on short-lived species such as excited

10.1021/cr980133r CCC: $35.00
Published on Web 09/28/1999

Katrin Kneipp received her Diploma, Ph.D. degree in Physics and habilitation from the Friedrich-Schiller University in Jena, Germany, and she received the facultas docendi from the Humboldt University in Berlin. After appointments at the university, in industry, and at the Academy of Sciences of the former German Democratic Republic, where she worked in the fields of optical spectroscopy, nonlinear optics, solid-state physics, and photochemistry, she joined the G. R. Harrison Spectroscopy Laboratory at the Massachusetts Institute of Technology as a Heisenberg Fellow. At present, she is an Oberingenieurin at the Technical University Berlin. Her current research interests include modern laser spectroscopic and nonlinear optics methods and their broad interdisciplinary applications.

Harald Kneipp received his Diploma from the Friedrich-Schiller University in Jena, Germany, and his Ph.D. degree in Physics from the Academy of Sciences of the former German Democratic Republic. He was appointed at the Central Institutes of Electron Physics and Optics and Spectroscopy of the Academy of Sciences, where he conducted research in the fields of plasma physics, laser physics, nonlinear optics, laser material processing, and medical laser applications. He worked on the development of dye lasers at Lambda Physik GmbH. He is now with Laser Analytical Systems GmbH, where he is engaged in diode-pumped solid-state lasers and cw second-harmonic generation. In his spare time, he is interested in applications of lasers in the frontiers of science and technology.

states and reaction intermediates (for example see ref 18).

The main advantage of Raman spectroscopy is its capability to provide rich information about the molecular structure of the sample. Recently, sophisticated data analysis techniques based on multivariate analysis have made it possible to exploit the full information content of Raman spectra and to draw conclusions about the chemical structure and composition of very complex systems such as biological materials.[19,20]

Despite all these favorable aspects, Raman spectroscopy has been considered to be more useful for structural analysis than for ultrasensitive trace

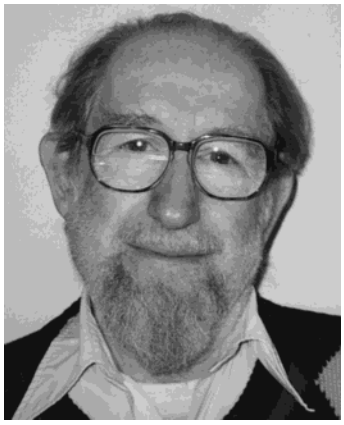

Dr. Irving Itzkan has been a Senior Scientist in the Massachusetts Institute of Technology Laser Biomedical Research Center since 1988. He received his Bachelors of Engineering Physics degree from Cornell University in 1952, his Masters of Electrical Engineering degree from Columbia University in 1961, and his Ph.D. degree in Physics from New York University in 1969. From 1956 to 1969 he was with Sperry Rand and from 1969 to 1985 with the Avco-Everett Research Laboratory where he worked on many different aspects of laser research. His principal present research interest involves using optical spectroscopy to diagnose disease.

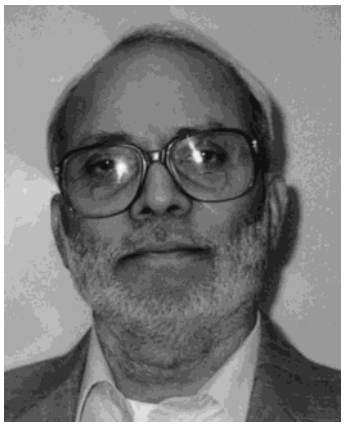

Ramachandra R. Dasari received his M.Sc. degree from Benaras Hindu University in 1956 and Ph.D. degree in Physics from Alighar Muslim University in 1960. He was Professor of Physics at Indian Institute of Technology Kanpur until 1978 and worked at the National Research Council, Ottawa, and University of British Columbia before joining the staff at Massachusetts Institute of Technology in 1980. His current research interests include cavity QED and single-atom laser characteristics and laser spectroscopy of biological tissue and ultrasensitive detection of carcinogenic protein adducts.

detection. The reason is the extremely small cross section for Raman scattering, typically $10^{-30}-10^{-25}$ cm^2/molecule, the larger values occurring only under favorable resonance Raman conditions. Such small Raman cross sections require a large number of molecules to achieve adequate conversion rates from excitation laser photons to Raman photons, thereby precluding the use of Raman spectroscopy as a method for ultrasensitive detection.

Up to now, optical trace detection with single-molecule sensitivity has been mainly based on laser-induced fluorescence (for reviews, see refs 21−25). Effective fluorescence cross sections can reach $\sim 10^{-16}$ cm^2/molecule for high quantum yield fluorophores. The fluorescence method provides ultrahigh sensitivity, but particularly at room temperature, the amount of molecular information which can be obtained from the broad fluorescence bands is limited.

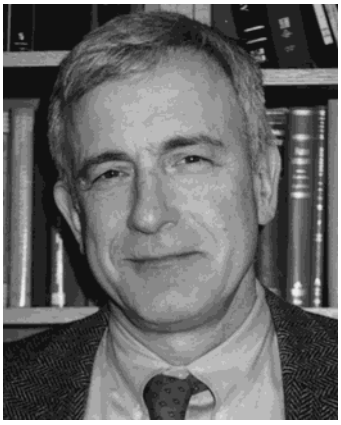

Michael S. Feld is a Professor of Physics at the Massachusetts Institute of Technology and directs the George R. Harrison Spectroscopy Laboratory there. He received his B.S. degree in Physics and M.S. degree in Humanities and Sciences in 1963 and his Ph.D. in Physics in 1967, all from Massachusetts Institute of Technology. He conducts research in biological physics and spectroscopy. He is also active in laser physics, particularly the coherent interaction of light with atomic and molecular systems, where his interests include cavity quantum electrodynamics, superradiance, and laser–nuclear physics. His publications include both theoretical and experimental topics. He has also done research in the history of science.

An important challenge facing analytical chemistry is not only detecting trace amounts of substances, but also identifying their chemical structure, for example by Raman scattering. Therefore, about 50 years after the discovery of the Raman effect, the novel phenomenon of a strongly increased Raman signal from molecules attached to metallic nanostructures attracted considerable attention from both basic and practical viewpoints[26,27] (for reviews, see refs 28−30). This effect, known as surface-enhanced Raman scattering (SERS), showed promise in overcoming the low-sensitivity problems inherent in Raman spectroscopy. As a spectroscopic tool, SERS has the potential to combine the sensitivity of fluorescence with the structural information content of Raman spectroscopy. When new methods for determining SERS enhancement factors resulted in unexpectedly large enhancement factors of at least 14 orders of magnitude, the discrepancy between Raman-scattering cross sections and fluorescence cross sections can be totally overcome[31] and detection of a single molecule with the high structural selectivity provided by its Raman spectrum became possible.[32,33]

Detecting single molecules and simultaneously identifying their chemical structures represents the ultimate limit in chemical analysis and is of great practical interest in many fields. For instance, further progress in human DNA sequence studies will mainly depend on developing methods for selective and rapid detection of four different single DNA bases.[34] Monitoring molecules and molecular interactions at the single-molecule level in cells or biological membranes and identifying single DNA fragments would be of great interest in the fields of medicine and pharmacology. Furthermore, the observation of Raman scattering of an individual molecule is of basic scientific interest and can provide insight into the nature of the effect and permit observations that cannot be made in an ensemble, due to averaging.

In this article, we shall discuss ultrasensitive Raman detection based on surface-enhanced Raman scattering. We shall take ultrasensitive in a rigorous light and restrict our review to Raman spectroscopy at the single-molecule level and at concentration ranges of target molecules on the order of femtomolar and smaller.[35,36]

As the prerequisite for such high Raman sensitivity, the effect of surface-enhanced Raman scattering will be briefly introduced, and the conditions for the occurrence of extremely strong SERS enhancement will be considered in section 2. Section 3 will deal with ultrasensitive Raman detection, in particular with single-molecule Raman spectroscopy. In section 4 we shall discuss the general potential and limitations of single-molecule Raman spectroscopy. Raman and fluorescence spectroscopy will be compared as tools for single-molecule detection. The potential of surface-enhanced nonlinear Raman spectroscopy for single-molecule detection will be briefly discussed.

2. Surface-Enhanced Raman Scattering (SERS)

2.1. Brief Introduction to the SERS Effect

In 1977, Van Duyne and Jeanmaire[26] and, independently, Albrecht and Creighton[27] concluded that the enormously strong Raman signal measured from pyridine on a rough silver electrode must be caused by a true enhancement of the Raman scattering efficiency itself and that it cannot be explained by an increase in surface area, i.e., an increase in the number of adsorbed molecules contributing to the Raman signal, as proposed earlier by Fleischman, Hendra, and McQuillan.[37] Within a few years, strongly enhanced Raman signals were verified for many different molecules, which had been attached to so-called "SERS-active substrates".[38] These SERS-active substrates are various metallic structures with sizes on the order of tens of nanometers. The most common types of SERS-active substrates exhibiting the largest effects are colloidal silver or gold particles in the 10−150 nm size range, silver or gold electrodes or evaporated films of these metals (for a general overview on SERS, see refs 28 and 29).

It is generally agreed that more than one effect contributes to the observed total enhancement of many orders of magnitude. Figure 1 presents a schematic of "normal" and surface-enhanced Raman scattering. In normal Raman scattering, the total Stokes Raman signal I_{NRS} is proportional to the Raman cross section σ^{R}_{free}, the excitation laser intensity $I(\nu_L)$, and the number of molecules N in the probed volume (see Figure 1, top). Because of the extremely small Raman cross sections, at least $\sim 10^8$ molecules are necessary to generate a measurable normal Raman scattering signal. In a SERS experiment (Figure 1, bottom), the molecules are attached to a metallic nanostructure which is a section of a cluster formed by aggregation of metal colloids; for comparison, see the electron micrographic views of colloidal gold and silver clusters in Figure 2. The surface-enhanced Stokes Raman signal I_{SERS} is proportional to the Raman cross section of the adsorbed molecule σ^{R}_{ads}, the excitation laser intensity $I(\nu_L)$, and

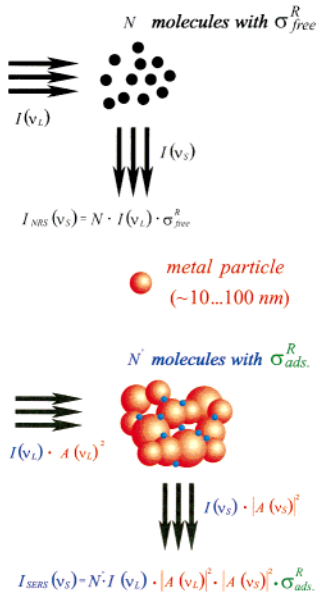

Figure 1. Comparison of "normal" (top) and surface-enhanced (bottom) Raman scattering. In Figure 1a, the conversion of laser light I_L into Stokes scattered light I_{NRS} is proportional to the Raman cross section σ^R_{free}, the excitation laser intensity I_L, and the number of target molecules N in the probed volume. Figure 1b displays a schematic of a SERS experiment. σ^R_{ads} describes the increased Raman cross section of the adsorbed molecule ("chemical" enhancement); $A(\nu_L)$ and $A(\nu_S)$ are the field enhancement factors at the laser and Stokes frequency, respectively; N' is the number of molecules involved in the SERS process.

the number of molecules which are involved in the SERS process N'. N' can be smaller than the number of molecules in the probed volume N.

The enhancement mechanisms are roughly divided into so-called "electromagnetic" field enhancement and "chemical first-layer" effects.[28,29,39] The latter effects include enhancement mechanism(s) of the Raman signal, which are related to specific interactions, i.e., electronic coupling between the molecule and metal, resulting in an "electronic" enhancement.[40] In Figure 1 (bottom), chemical SERS enhancement is expressed as an increased Raman cross section σ^R_{ads} of the adsorbed molecule compared to the cross section in a normal Raman experiment σ^R_{free}. Possible electronic SERS mechanisms involve a resonance Raman effect due to a new metal−molecule charge-transfer electronic transition[28,41] or a dynamic charge transfer between the metal and molecule, which can be described by the following four steps:[39,40] (a) photon annihilation, excitation of an electron into a hot electron state, (b) transfer of the hot electron into the LUMO of the molecule, (c) transfer of the hot electron from the LUMO (with changed normal coordinates of some internal molecular vibrations) back to the metal, (d) return of the electron to its initial state and Stokes photon creation. "Roughness" seems to play an important role by providing pathways for the hot electrons to the molecule. The magnitude of chemical enhancement has been estimated to reach not more than factors of 10−100.[28]

In Figure 1 (bottom), $A(\nu_L)$ and $A(\nu_S)$ represent field enhancement factors of the laser and Stokes fields.

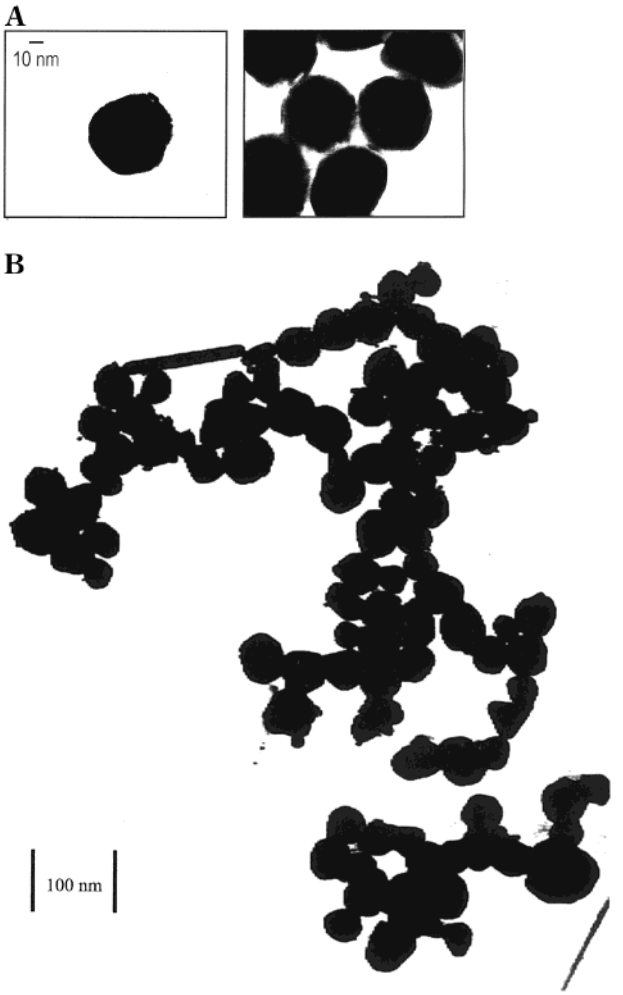

Figure 2. Electron micrographs of typical colloidal gold and silver structures used in SERS experiments. (a) Colloidal gold particles in the isolated stage and aggregated stage after addition of NaCl. (Reprinted with permission from ref 53. Copyright 1998 Society for Applied Spectroscopy.) (b) Typical colloidal silver clusters exhibiting extremely strong SERS enhancement.

The electromagnetic or field enhancement factors arise from enhanced local optical fields at the place of the molecule nearby the metal surface due to excitation of electromagnetic resonances, which appear due to collective excitation of conduction electrons in the small metallic structures, also called surface plasmon resonances. Because the excitation field, as well as the Raman scattered field, contributes to this enhancement, the SERS signal is proportional to the fourth power of the field enhancement factor. Electromagnetic field enhancement has been calculated for isolated single colloidal silver and gold spheroids.[42,43] Maximum values for electromagnetic enhancement are on the order of 10^6−10^7 for isolated particles of these metals. Theories for surface plasmon-based field enhancement were also developed for two coupled small metal particles or bumps. Closely spaced interacting particles seem to provide extra field enhancement, particularly near the gap sites between two particles in proximity, resulting in electromagnetic SERS enhancement factors up to 10^8.[44−49] Theory also predicts strong enhancement of electromagnetic fields for sharp features and large curvature regions, which may exist on silver and gold

nanostructures (for more information on electromagnetic SERS enhancement, see refs 28, 29, and 47).

Surface plasmon resonance can also explain the initial discovery of surface-enhanced Raman scattering. This observation was possible because the blue and green emission lines of the Ar^+ laser just fell in the excitation range of surface plasmons of the bumps on the electrochemically roughened silver electrode. In general, the plasmon resonance frequency depends on the size, shape, and, of course, the material of the metallic nanoparticles and their environment. These sharp resonances were already exploited hundreds of years ago, when small metal particles were embedded in glass to generate the brilliant colors of the windows in old cathedrals.[50]

However, in many experiments, SERS-active substrates consist of a collection of nanoparticles exhibiting fractal properties, such as colloidal clusters formed by aggregation of colloidal particles or metal island films.[51−54] In experiments performed on cluster structures, "classical" electromagnetic field enhancement, which is based on the electromagnetic response of isolated individual particles, is not valid and estimates of electromagnetic SERS enhancement must be based on the exciting optical properties of fractal small-particle composites.[55] In such structures, the individual dipole oscillators of the small isolated particles couple, thereby generating normal modes of plasmon excitation that embrace the cluster. In general, the excitation is not distributed uniformly over the entire cluster but tends to be spatially localized in so-called "hot" areas.[55−62] The nonuniform distribution of excitation results from the fractal geometry of the clusters, where the excitations are considered neither as surface plasmon polaritons nor as independent localized surface plasmons.

As discussed in the previous paragraph for individual silver or gold particles, at the surface plasmon resonance, the electromagnetic field intensities in the vicinity of these particles can be strongly enhanced. The same effect is also true for the resonances with the electromagnetic excitations of clusters. When optical excitation is localized in "hot spots", extremely large electromagnetic field enhancement was theoretically predicted for these areas by Shalaev, Moskovits, and co-workers.[56−59] The size of the "hot spots" is predicted to be often much smaller than the wavelength; their locations depend strongly on the geometry of the fractal object and on the excitation wavelength and polarization. Figure 3a illustrates the behavior of field distribution above a fractal cluster structure by showing calculated maps of the square modulus of the local field 100 nm above an assembly of silver colloidal clusters. The false-color images of the electromagnetic field distribution were generated for various excitation wavelengths in the visible and near-infrared region. The topographic image of the simulated collection of silver clusters used for the field estimates is shown in the upper right-hand corner of Figure 3 and is very similar to the actual clusters used in SERS experiments (see for instance the collection of silver particles shown in Figure 2). Figure 3 displays the inhomogeneous field distribution over a cluster structure. Simultaneously, it demonstrates that the same area can be a hot spot or a "could" zone, depending on the excitation wavelength used. In ref 62 the electromagnetic field above a self-affine fractal surface was probed using the high lateral resolution of an optical near-field experiment. The self-affine fractal surface was prepared by gravitationally depositing colloidal silver particle aggregates out of solution onto a coverslide. Near-field spectra were measured for various wavelength of an Ar^+-laser pumped Ti:sapphire laser. The images were recorded with a sharpened fiber tip scanning 25 nm above the surface. The measured pattern of hot spots and their strong spectral dependence are in qualitative agreement with the predicted electromagnetic field intensity distributions shown in Figure 3.[62] Moreover, the local field intensities very close to the surface are predicted to be much more heterogeneous than in the 25 nm distance so that the variation in field intensities can exceed 10^5, implying local electromagnetic SERS enhancement factors in excess of 10^{10}.

2.2. SERS Enhancement Factors and Effective SERS Cross Sections

The size of the enhancement factor or, in other words, the size of the effective SERS cross section is a key question for application of SERS as tool for ultrasensitive detection. The effective cross section must be high enough to be able to generate a detectable Raman signal from a few molecules.

In the first SERS experiments, Van Duyne and coworker estimated enhancement factors on the order of 10^5-10^6 for pyridine on rough silver electrodes. The value was derived from a comparison between surface-enhanced and "bulk" Raman signals of pyridine, taking into account the different number of molecules on the electrode and in solution. The size of the enhancement was found to be dependent on electrode "roughness", which suggests a strong electromagnetic field enhancement. On the other hand, the experimental observation of the dependence of the enhancement factor on the electrode potential is an indication that "chemical" enhancement must be operative as well.

For excitation laser wavelengths in resonance with the absorption band of target dyes, surface-enhanced resonance Raman scattering (SERRS) has been obtained. In such experiments, a superposition of surface enhancement and the resonance Raman effect can result in strong total enhancement factors or effective Raman cross sections. Total enhancement factors on the order of approximately 10^{10} for rhodamine 6G and other dyes adsorbed on colloidal silver and excited under molecular resonance conditions have been reported by several authors in independent experiments.[63−72] In ref 72 Raman cross sections of 10^{-18} cm^2 were obtained from a comparison of the intensities of SERRS with solution fluorescence of rhodamine 6G. An alternative way for a rough estimate of SERS enhancement factors is shown in Figure 4, where the enhancement factor of rhodamine 6G in silver colloidal solution was determined by comparing the intensity of the nonenhanced methanol Raman line to the enhanced Raman lines

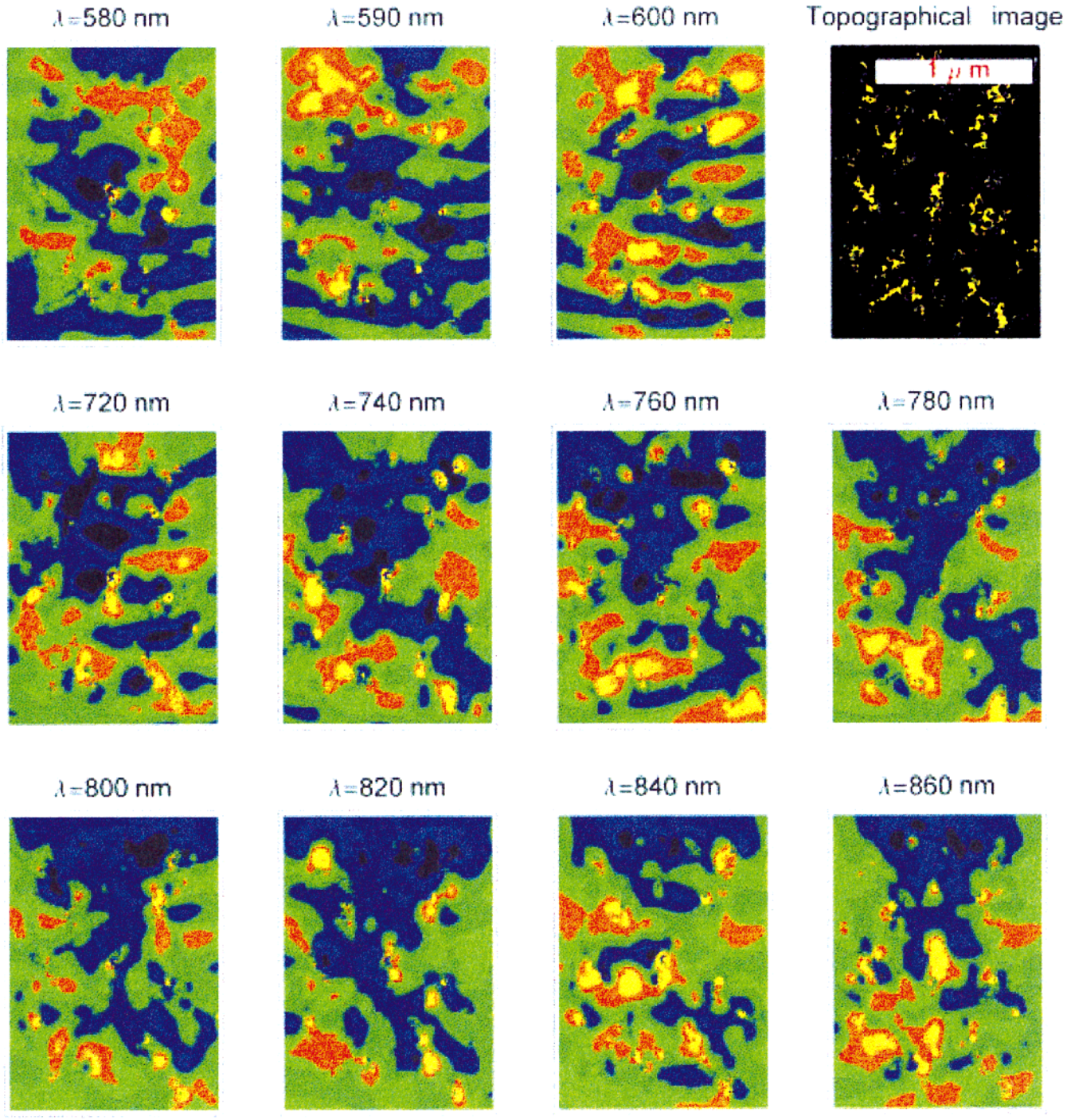

Figure 3. Calculated near-field false-color images computed 100 nm above the topographical silver cluster image shown in the upper right-hand corner. Maximum intensity is shown as yellow and the minimum is black; the intensity range covers approximately a factor 4. (Reprinted with permission from ref 62. Copyright 1999 American Institute of Physics.)

of rhodamine 6G, taking into account the different concentrations of both compounds (8×10^{-11} M rhodamine 6G and 5 M methanol). The total enhancement factor was estimated to be on the order of 5×10^{11}.[73]

In general, all estimates of enhancement factors based on the comparison of SERS intensity with fluorescence intensity or with normal Raman intensity suffer from the fact that we do not know the number of target molecules really involved in the SERS process which contribute to the Raman signal. The assumption that nearly all molecules in the SERS sample contribute in a similar way will result in the estimate of a minimum (average) cross section.

To avoid this problem, we applied a different approach, in which surface-enhanced Stokes and anti-Stokes Raman scattering is used to extract information on the effective SERS cross section.[31] Figure 5 shows surface-enhanced Raman spectra of crystal violet on silver colloidal clusters collected at the Stokes and anti-Stokes side of the near-infrared excitation laser. The Stokes and anti-Stokes Raman process starts from the ground and first excited vibrational state, respectively (see sketch in Figure

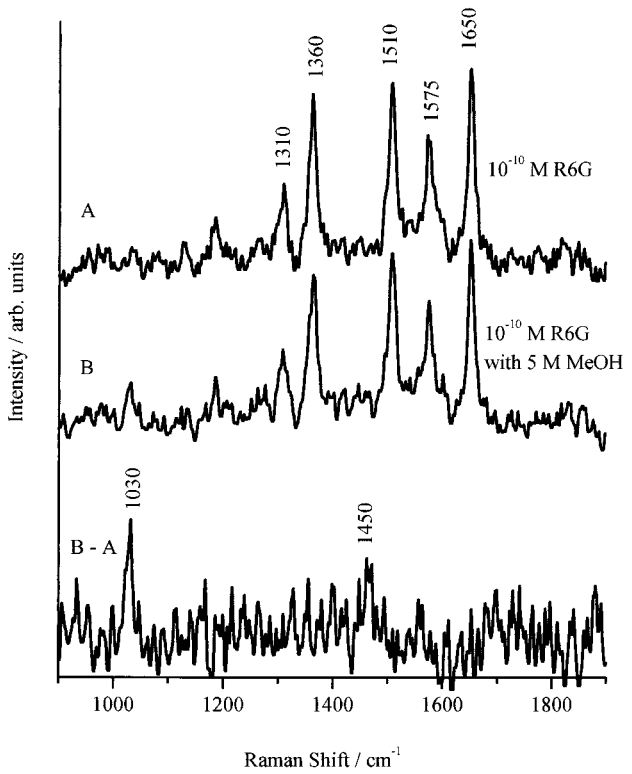

Figure 4. SERRS spectrum from 8×10^{-11} M rhodamine 6G in silver colloidal solution (top), with addition of 5 M methanol (middle). Spectra were measured using 514.5 nm resonant excitation; laser intensity was ca. 10^3 W/cm^2. No fluorescence was obtained at such low concentration because all dye molecules can find a place on the colloidal silver particles where the fluorescence is quenched. The bottom curve depicts the exact subtraction of the top curve from the middle one and shows only the methanol lines. The methanol Raman signal is not enhanced on colloidal silver and shows a Raman cross section on the order of 10^{-30} cm^2/molecule.[133]

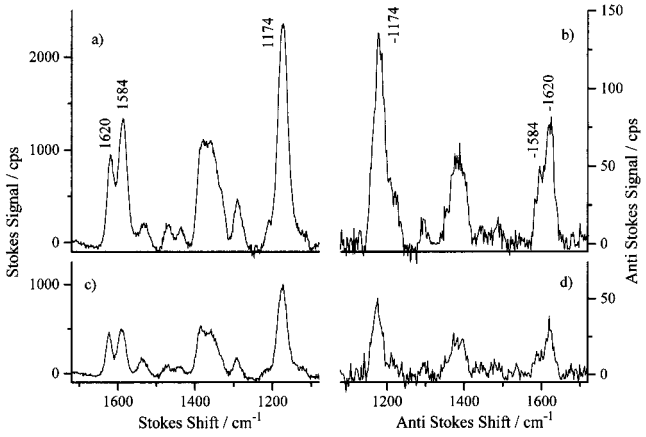

Figure 5. Stokes and anti-Stokes SERS spectra of crystal violet adsorbed on colloidal silver clusters of different sizes; spectra a and b are measured from a 1 μm colloidal cluster. Spectra c and d are measured from a collection of small 100−500 nm clusters. Spectra were collected in 1 s using approximately 10^5 W/cm^2 excitation at 830 nm.

6). The anti-Stokes to Stokes signal ratio is determined by the ratio of the number of molecules in the first excited vibrational level, N_1, and in the vibrational ground state, N_0. In a "normal" Raman experiment, this ratio is determined by the Boltzmann population and, therefore, high-frequency vibrational modes appear at an extremely low signal level in the anti-Stokes spectra. A very strong surface-enhanced Raman process can measurably populate the first excited vibrational level in excess of the Boltzmann population (see estimates below). This is demonstrated by Figure 5, where the relative intensities within the Stokes and anti-Stokes spectra are very similar, including the higher frequency modes. This behavior indicates that anti-Stokes scattering arises from vibrational levels that are mainly populated by the SERS process and not by thermal population. This "vibrational population pumping", which is reflected in deviation of the anti-Stokes to Stokes signal ratio from that expected from a Boltzmann population, allows a rough estimate of the size of Raman cross sections effective in "pumping". Figure 6 illustrates the estimate of the effective SERS cross section from anti-Stokes to Stokes SERS signal ratio using a straightforward method based on the pumping of molecules to the first excited vibrational states via the strongly enhanced Raman process.[31] As the first equation in Figure 6 shows, the excited vibrational level is populated by Stokes scattering and depopulated by anti-Stokes scattering and spontaneous decay (τ_1). Assuming steady state and weak saturation, a simple theoretical estimate for the anti-Stokes to Stokes SERS signal ratio I_{aS}^{SERS}/I_s^{SERS} can be derived as shown in Figure 6. The first term on the right-hand side of the equation for I_{aS}^{SERS}/I_s^{SERS} describes the "SERS population" of the first excited vibrational state in excess of the Boltzmann population. In normal Raman scattering, this term can be neglected compared to the thermal population.[74] However, in SERS experiments, significant deviations of anti-Stokes to Stokes SERS signal ratios from thermal population are measured at relatively low excitation intensities. To account for the anti-Stokes to Stokes signal ratios experimentally obtained, the product of the cross section and vibrational lifetime, $\sigma^{SERS}(\nu_m)\tau_1(\nu_m)$, must be on the order of 10^{-27} cm^2 s. Assuming vibrational lifetimes of the order of 10 ps,[75] the surface-enhanced Raman cross section is then estimated to be at least $\sim 10^{-16}$ cm^2/molecule. It should be noted that this estimate is an approximation and the enhancement factor and SERS cross section can include uncertainties of an order of magnitude.

To make the large cross sections inferred from vibrational pumping consistent with the level of the observed SERS Stokes signal, we must draw the conclusion that the number of molecules which are involved in the SERS process at the extremely high enhancement level must be very small.[31] Depending on the concentration of the colloids, this number was found to be between 10^{-13} and 10^{-10} M concentration, which in some experiments is ~0.01% of the molecules present in the probed volume.[76]

Cross sections of at least 10^{-16} cm^2/molecule were inferred from vibrational pumping experiments for rhodamine 6G and other dyes,[31,77] as well as for adenine.[52] It should be noted that the cross sections were derived from experiments performed at near-infrared excitation. The 830 nm laser light is clearly

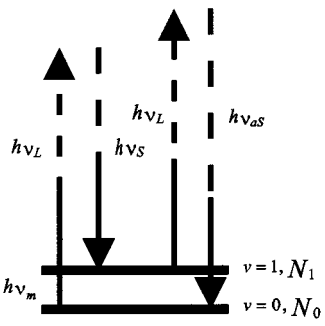

$$\frac{dN_1}{dt} = (N_0 - N_1)\sigma^{SERS} n_L - \frac{N_1}{\tau_1}$$

σ^{SERS} : effective SERS cross section

τ_1 : lifetime of the first excited vibrational state

n_L : photon flux density of the excitation laser

with steady state and weak saturation ($\sigma^{SERS}\ \tau_1\ n_L << 1$)

$$I_{aS}^{SERS} / I_S^{SERS} = \underbrace{\sigma^{SERS}\ \tau_1\ n_L}_{\text{SERS pumping}} + \underbrace{e^{-h\nu_m/kT}}_{\text{Boltzmann population}}$$

Figure 6. Pumping of the first excited vibrational level due to the strong Raman process and estimate of the effective SERS cross section from anti-Stokes to Stokes SERS signal ratio (for explanation, see text).

far away from any electronic transitions in the target molecules, particularly in the case of adenine, thereby excluding a contribution to the enhancement due to resonance Raman scattering (RRS). The extremely large enhancement factors seem to be related to the existence of colloidal clusters.[52,77] Giant local fields in the hot zones of these fractal structures[59,62,78] might provide a rationale for the large nonresonant SERS cross sections, but the experimental results did not rule out a "chemical contribution" to the total enhancement.

Studies on colloidal gold cluster showed the same extremely large effective SERS cross section corresponding to an enhancement level of about 10^{14}. The strong similarity between gold and silver as SERS-active substrates appears only in the near-infrared region where colloidal clusters are efficient SERS-active structures. Spatially isolated spherical colloidal silver and gold particles show very different SERS enhancement for excitation wavelengths at the appropriate single-particle plasmon resonances. In agreement with electromagnetic estimates, small isolated colloidal gold spheres show maximum enhancement factors on the order of 10^3 at 514 nm compared to enhancement factors of about 10^6 obtained for isolated small silver spheres for excitation wavelengths at the appropriate single-particle plasmon resonance at 407 nm.[52,53]

Figure 2b shows an electron micrograph of a typical colloidal silver structure which exhibited a strong SERS enhancement at near-infrared excitation. In agreement with theory, after exceeding the critical size of the clusters, the enhancement factor is independent of the size of the cluster.[52,53] This is demonstrated in Figure 5. Spectra a and b in this figure are collected from a 1.2 μm spot on a 10-μm colloidal cluster; spectra c and d are from a collection of small 100−500 nm clusters. Different numbers of molecules contribute to the SERS signal measured from those two different regions. Therefore, different SERS signal heights were collected from both regions. However, the ratios between anti-Stokes and Stokes SERS signals are constant within the accuracy of our measurement. That means that the vibrational pumping rate or, in other words, the SERS enhancement factor must be the same at all places, independent of the size of the colloidal clusters.

The important role of field enhancement is also supported by strongly enhanced hyper-Raman scattering[79−83] up to 20 orders of magnitude,[84] which can be explained by a very strong electromagnetic field enhancement. In the framework of a field enhancement model, hyper-Raman scattering is surface enhanced to a greater extent than "normal" Raman scattering since it nonlinearly depends on the (enhanced) laser field.

In 1997, Nie and Emory confirmed the existence of Raman enhancement factors on the order of 10^{14}−10^{15} for rhodamine 6G molecules on colloidal silver particles under resonant excitation.[33] By screening a large number of individual silver particles immobilized on a glass slide, the authors found a small number of nanoparticles exhibiting unusually high enhancement efficiencies, called hot particles. Figure 7 shows atomic force microscopy (AFM) images of typical hot particles. The size of the SERRS cross section or enhancement factor was determined by a comparison of the SERRS signal of rhodamine 6G adsorbed on a hot silver particle with the fluorescence signal of rhodamine 6G molecules adsorbed on glass. Nie and Emory attribute their finding to the removal of two population averaging effects. The intrinsic enhancement effect can be 10^6−10^7 times larger than the ensemble average value because only 1 out of 100−1000 silver particles are hot particles (particle-averaging factor 10^2−10^3) and only 1 out of 10 000 surface sites show efficient enhancement (molecule averaging factor 10^4). The authors stated that such an enormous degree of signal amplification can be obtained by exploiting the surface-enhanced Raman

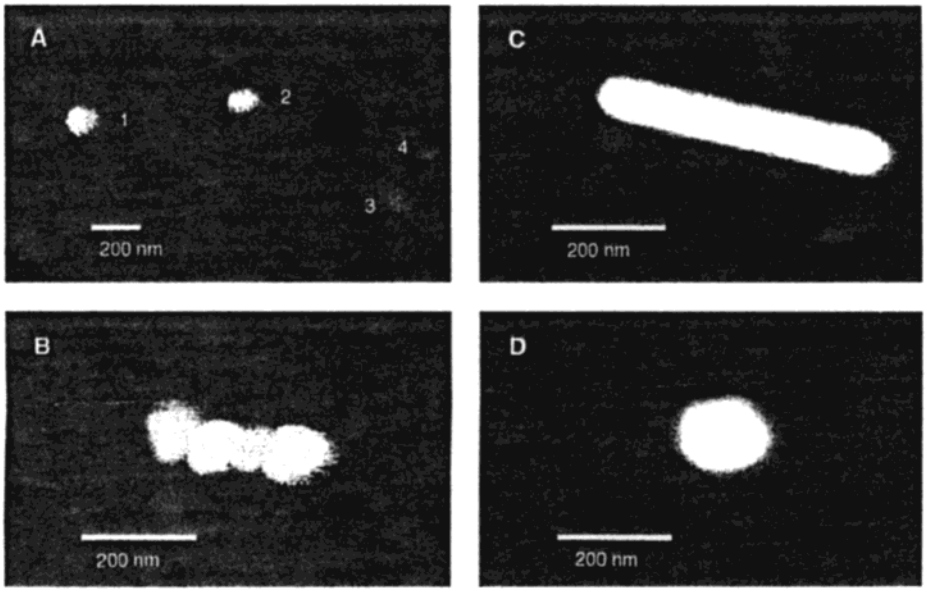

Figure 7. Tapping-mode AFM images of typical hot particles: (A) four single nanoparticles. Particles 1 and 2 were highly efficient for Raman enhancement, but particles 3 and 4 were not. (B) Close-up image of a hot aggregate containing four linearly arranged particles. (C) Close-up image of a rod-shaped hot particle. (D) Close-up image of a faceted hot particle. (Reprinted with permission from ref 33. Copyright 1997 American Association for the Advancement of Science.)

effect and the resonance Raman effect. In a more detailed study of hot particles, Nie and co-workers found that different particles are hot for special wavelengths.[85] So, in a very heterogeneous collection of chemically prepared silver particles, only a few particles have an optimum size and shape for a given excitation wavelength. The strong dependence of the SERS effect on the excitation frequency for molecules adsorbed on isolated colloidal silver particles of different sizes and shapes is demonstrated in Figure 8. Figure 8a shows the multicolor Raman image which was collected from different isolated nanoparticles using multiwavelength excitation. Single particles at sizes between 70 and 140 nm are detected as diffraction-limited spots in far-field optical microscopy. The SERS signals of the different particles appear at the different resonant wavelengths of the different particles. In general, electromagnetic theories for isolated spheroids explain the correlation between the size of hot particles and their optimum excitation wavelength but give maximum field enhancement factors on the order of 10^6-10^7.[43,47] Assuming a resonance Raman effect contribution of about 10^4-10^5, such an electromagnetic enhancement level does not explain the enhancement factor of $10^{14}-10^{15}$ stated as enhancement factors for single silver particles.[33] One may have to consider either additional field enhancement mechanisms, related to sharp edges and kinks (see shapes of hot particles in Figure 7), or an additional electronic enhancement mechanism.

Very large surface enhancement factors have been reported also for the resonance Raman spectra of hemoglobin on optically "hot" silver nanoparticles[86] (see also section 3.2.). Scanning electron and atomic force microscopy images of these "hot sites" revealed dimers, or sometimes larger aggregates, of closely spaced Ag particles with typical dimensions of ~100 nm. No isolated Ag particles were found to be "hot". The large enhancement was ascribed to a strong field enhancement at the midpoint between two Ag spheres.

Recently, Brus and co-workers repeated surface-enhanced resonance Raman experiments on rhodamine 6G adsorbed on silver colloidal particles.[87] For sample preparation, the authors followed the general procedures described in ref 33. SERRS spectra were measured from rhodamine 6G on immobilized silver colloidal particles using 514 nm excitation. The magnitude of the SERRS cross section was determined by comparing the SERRS count rate with the fluorescence count rate for single carbocyanine dye molecules (DiI). SERRS cross sections measured from 100 SERS-active silver particles showed a wide distribution with an average of 2×10^{-14} cm^2. This value is somewhat higher than the approximate value in Nie's and Emory's experiments. It is interesting to note that the large SERS enhancement was obtained from molecules on small colloidal aggregates, created by salt-induced aggregation and not from single colloidal particles as in Nie's and Emory's experiments.

In ref 87, in addition to SERRS studies, Rayleigh scattering is used to probe the electromagnetic resonances of the silver particles. Rayleigh scattering images were obtained using an inverted optical microscope equipped with a dark-field condenser and a tungsten lamp. As a pendant to the multicolor SERRS image, Figure 8b shows the multicolor Rayleigh image collected from many isolated silver particles. Most of the particles in Figure 8b were single particles of varying sizes and shapes including spheres and rod-shaped particles. Each particle generates a scattering signal at its own resonance frequency. A more detailed study of the Rayleigh spectra of individual silver particles shows single peaks centered at different wavelengths depending on the shape and size of the particles. Small aggregates formed by a few individual colloids show

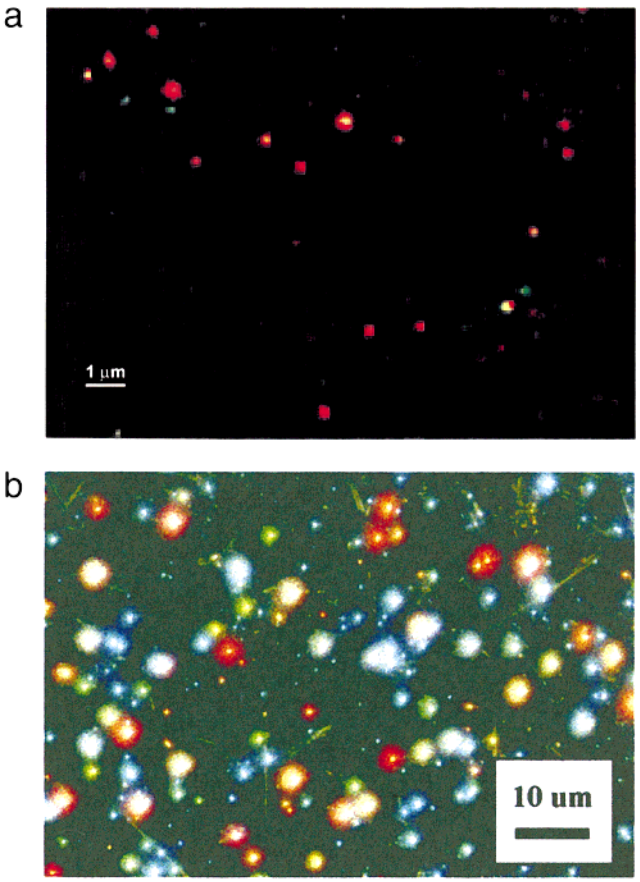

Figure 8. (a) Multicolor Raman image of Ag nanoparticles excited with a mercury lamp at 490 and 570 nm. The probe molecule is bis(4-bipyridyl)ethylene (BPE). The green, red, and yellow signals correspond to 70 nm particles (excited at 490 nm), 140 nm particles (excited at 570 nm), and intermediate-sized particles or nanoaggregates (excited at both 490 and 570 nm), respectively. (b) Multicolor Rayleigh image of Ag nanoparticles excited with a tungsten lamp. For rough orientation, the blue particles correspond to spherical Ag particles with a size of approximately 50 nm or to smaller nonspherical particles and red images come from particles with very high axial ratios, such as rods. (Reprinted with permission from refs 85 and 87. Copyright 1998 American Chemical Society.)

more complex and broad spectra. An interesting experimental finding is that there is no correlation between the intensity of the SERRS signal of rhodamine 6G adsorbed on these silver particles and the Rayleigh scattering intensity from the 514 nm excitation laser. The authors discuss the extremely large SERRS enhancement in terms of an additional "electronic" enhancement[39,40] for rhodamine 6G molecules adsorbed at special sites. In conjunction with the rhodamine 6G SERRS signal, a continuum emission appears. This underlying white continuum has been reported in many SERS studies and has been discussed to be directly related to the "electronic" SERS enhancement.[39,40]

3. Single-Molecule Raman Spectroscopy

3.1. Application of SERS for Trace Analysis down to an Approximately 100 Molecule Detection Limit

In the middle of the 1980s, despite the relatively poor understanding of the effect and despite the poor quantitative estimates of total enhancement factors, surface-enhanced Raman scattering generated growing interest as a useful tool for trace analysis. The possibilities of SERS for detecting minimum amounts of substances down to picogram detection limits were demonstrated for a variety of molecules of environmental, technical, biomedical, and pharmaceutical interest.[88−95] For example, the separation and determination of adenine, guanine, hypoxanthine, and xanthine was performed using liquid chromatography in combination with SERS.[96] The neurotransmitter dopamine was detected in 10^{-7} M concentration by SERS on a silver electrode.[93]

An important aspect which aided in the trace detection of dyes and related molecules was the quenching of fluorescence, which occurs due to additional new relaxation channels to the metal surface for the electronic excitation. This allowed the detection of excellent vibrational spectra over wide frequency ranges from minimum amounts of substances that were not previously accessible to Raman studies until that time because of their strong fluorescence signal.[67,71,72,97−100] To demonstrate the very good structural selectivity, Figure 9 shows SERRS spectra of 8 very similar polymethine dyes used as spectral sensitizers in photographic films. The dyes cannot be distinguished by absorption or fluorescence spectra, but they can be distinguished by their SERRS spectra.[101] In ref 102 the authors report molecularly distinct SERRS spectra of 23 azo dyes.

A key problem in analytical application of SERS is developing stable and reproducible SERS-active substrates that provide a large enhancement factor. Silver, gold, and copper have been prepared in a variety of ways to generate SERS-active substrates for applications in various environments. SERS substrates used for analytical applications include roughed silver electrodes,[103] silver films made by vapor deposition[104] or photoreduction,[105] silver and gold colloidal particles self-assembled into polymer-coated substrates,[106] electrochemically prepared silver oxide,[107] silver particles layered onto etched polymer substrates,[108] and colloidal metal particles in hydrosols.[109,110] Common SERS-active substrates for analytical use provide comparatively low enhancement factors ranging between 10^3 and 10^6, which can be increased by exploitation of the resonance Raman effect if the target molecule has electronic transitions in the range of the excitation laser. For typical SERS-active substrates, calibration plots exhibit a linear response over 2−3 orders of magnitude.[88,94,111] The precision expected from a SERS experiment is typically 15−20% relative standard deviation.[35,108]

An overview on SERS trace analytical studies at the $\sim 10^{-7}-10^{-12}$ M level approaching detection limits of approximately 10^4 molecules is given in ref 35.

As discussed in section 2, colloidal silver or gold particles, particularly their aggregates, provide very high SERS enhancement levels. For trace analytical application, colloidal solutions containing small aggregates in sizes between about 100 and 1000 nm are very useful SERS-active substrates. At very low analyte concentrations (ca. 10^{-11} M and lower) when the number of target molecules becomes comparable

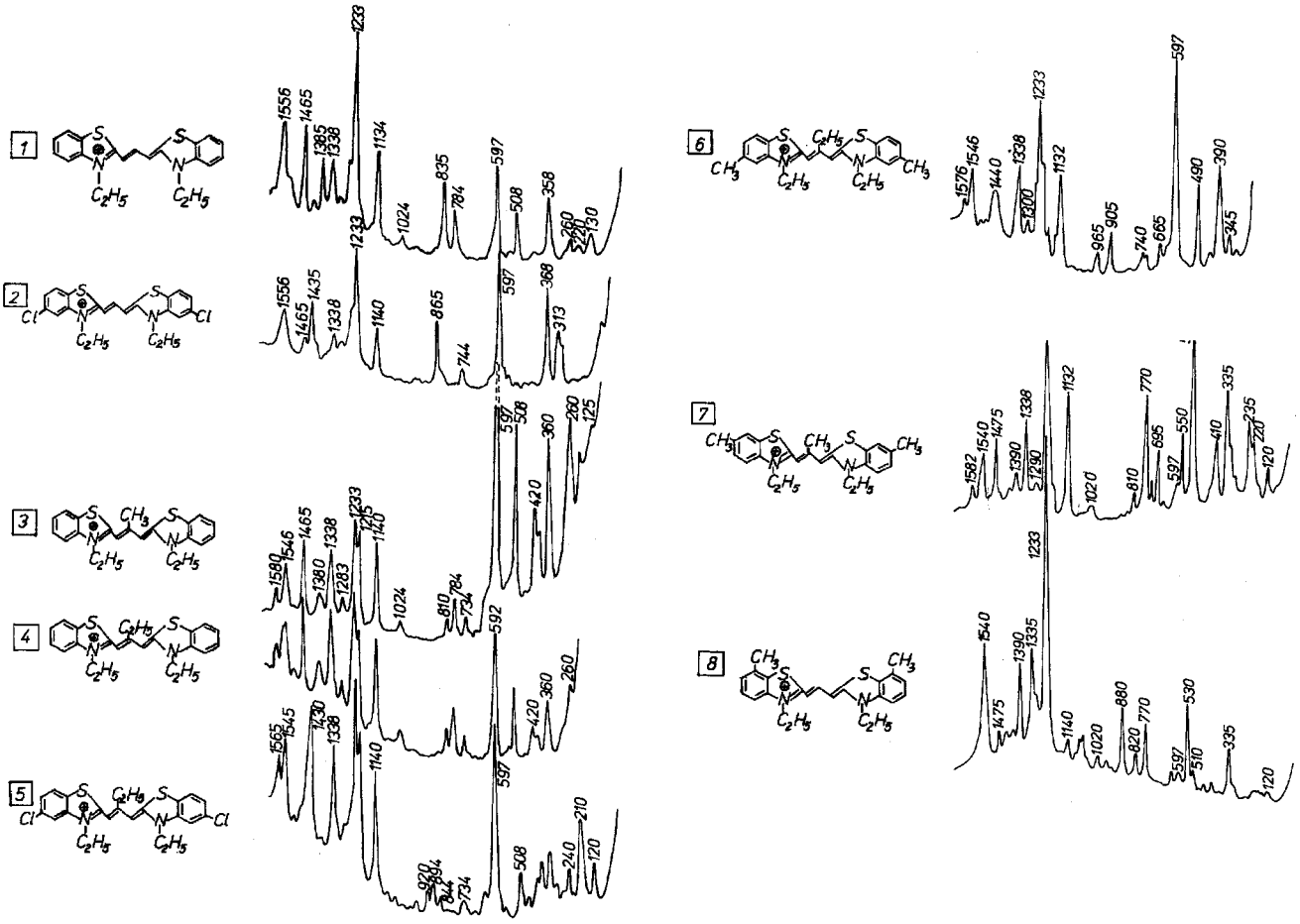

Figure 9. SERRS spectra of 10^{-8} M polymethine dyes in silver colloidal solution. The dyes show the same absorption or fluorescence spectra, but they can be distinguished by their SERRS signals.[101]

to or smaller than the number of the silver particles, no analyte-induced aggregation can occur and the SERS spectra show a very good reproducibility.[73,112]

In 1988, SERRS spectra from rhodamine 6G in slightly aggregated and NaCl-activated silver colloidal solution were collected from a 7×10^{-14} M dye.[113] SERRS signals were reproducible within 15% and showed a linear plot vs dye concentration between 7×10^{-11} and 7×10^{-14} M. Saturation of the SERRS signal vs rhodamine 6G concentration set in when the ratio of R6G molecule to small colloidal silver clusters was about 3:1. Since the scattering volume in that experiment was smaller than 10 nL, the detection limit was on the order of 100 R6G molecules. Despite resonant excitation, rhodamine 6G molecules showed a relatively high stability on the silver colloids because of the strong quenching of the excited electronic states. The results were confirmed in 1995 where we collected SERRS signals from 60 R6G molecules. Spectra were measured down to 8×10^{-16} M dye concentration in aqueous silver colloidal solution.[73]

Also in 1988, SERS signals of approximately 600 pyridine molecules were measured on a rough silver electrode with extrapolation to detection limits of about 100 molecules.[114] Figure 10 shows pyridine/Ag SERS spectra as a function of pyridine solution concentration.[115] The 1008 cm^{-1} band of pyridine could still be detected at a bulk concentration of 5×10^{-5} M. It was estimated that this bulk concentration produced a coverage corresponding to 1×10^{-5} ML corresponding ca. 600 molecules inside the 2.1 μm radius laser spot size.

Reference 116 describes a flow injection sampling system to analyze molecules in aqueous colloidal solutions. Major spectral peaks of crystal violet were observable down to concentrations of 1×10^{-12} M using SERRS. Detection limits were estimated to be on the order of 600 molecules based on a 1 nL sampled volume.

In ref 117 the authors describe detection of rhodamine 6G adsorbed on silver colloidal aggregates at concentration levels which are equivalent to 6.87×10^{-18} M in solution. This corresponds to 35−200 molecules in the beam at any one time.

In ref 118 resonance near-field surface-enhanced Raman spectra have been reported which were recorded from approximately 300 dye molecules that were located underneath the tip.

3.2. Raman Detection of a Single Molecule

In a recent review on optical studies of single molecules at room temperature, the authors state that any photostable molecule with an extinction coefficient larger than about 10^4 (10^4 L/mol cm corresponds to an absorption cross section of ca. 4×10^{-17} cm^2/molecule) and a fluorescence quantum efficiency greater than 0.1 can be studied as single using its fluorescence signal.[25] Assuming comparable

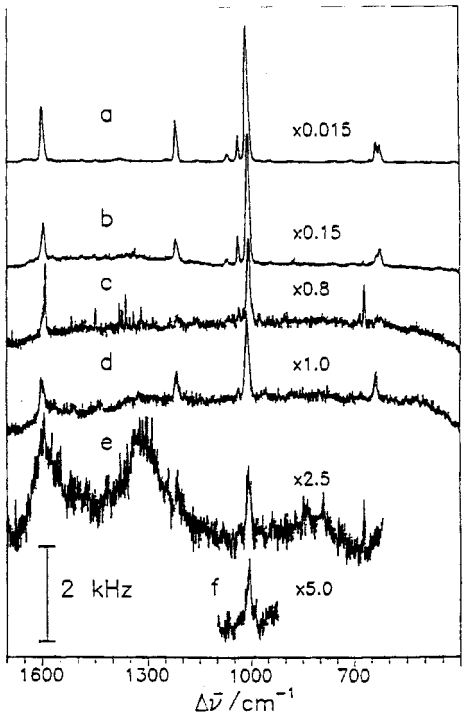

Figure 10. Pyridine/Ag SR−SERS spectra as a function of pyridine solution concentration: (a) 500 mM, (b) 50 mM, (c) 5 mM, (d) 0.5 mM, (e) 0.05 mM, (f) 0.005 mM. Spectra were recorded using 15 mW excitation laser at 647 nm, $E = -0.7$ V vs Ag/AgCl for all spectra. (Reprinted with permission from ref 115.)

signal-to-background ratios in SERS and fluorescence experiments, transformed to Raman scattering, that means, that an effective Raman cross sections larger than 4×10^{-18} cm^2/molecule should allow single-molecule detection using Raman scattering.

Two methods have been used to achieve single-molecule sensitivity in a SERS experiment. One is based on the extremely large effective SERS cross sections obtained on colloidal clusters at near-infrared excitation.[31,32,52,77] The effect is nonresonant to the optical transitions in the target molecule. In the second way, the surface-enhanced resonance Raman experiments are improved to single-nanoparticle−single-molecule experiments.[33,86,87] By removing averaging effects for selected single "hot" colloidal silver particles, the authors find effective SERS cross sections similar to or even larger than those obtained from vibrational pumping experiments on colloidal clusters.

Figure 11 shows a schematic of a typical single-molecule SERS experiment performed in silver or gold colloidal solution.[32,52,77,119] Spectra are excited by an argon-ion laser pumped cw Ti:sapphire laser operating at 830 nm with a power of about 100−200 mW at the sample. A microscope attachment is used for laser excitation and collection of the Raman scattered light. The analyte is provided as a solution at concentrations smaller 10^{-11} M, which is added to the solution of small colloidal clusters. At such low concentrations, it is very unlikely that molecular aggregates exist in the analyte solution. Concentration ratios of silver clusters and target molecules of at least 10 make it unlikely that more than one analyte molecule will be attached to the same colloidal cluster, avoiding formation of aggregates of the target molecule on the surface. Addition of the analyte at such a low concentration does not induce coagulation of the colloidal particles/colloidal clusters, avoiding formation of larger clusters.[120] The described procedure results in individual single molecules that

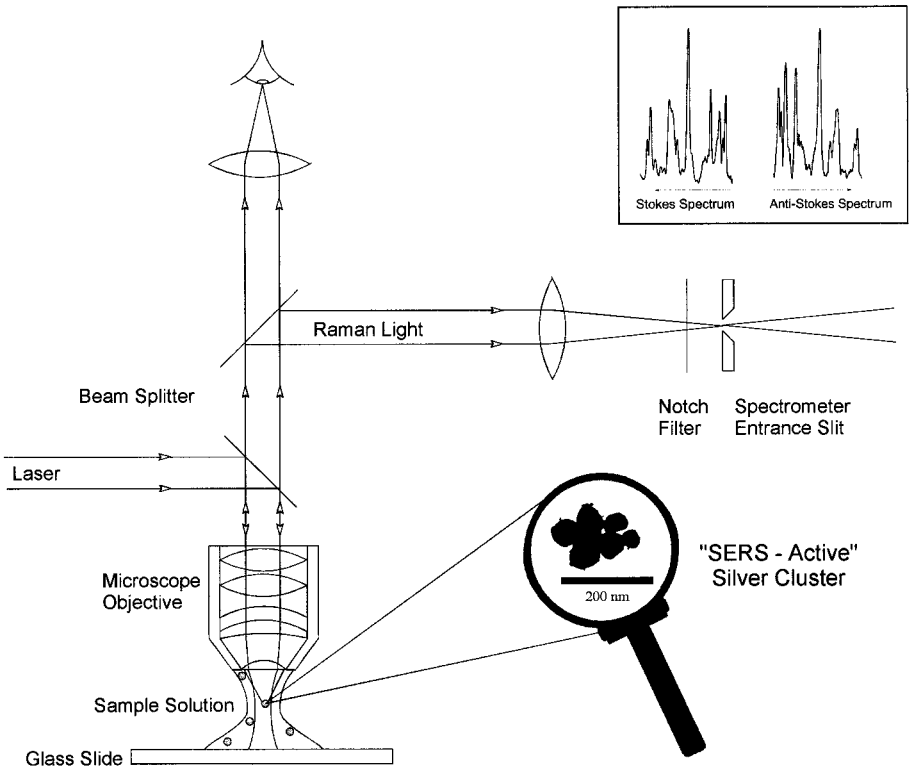

Figure 11. Schematic experimental set up for single-molecule SERS. The insert shows an electron micrograph of typical SERS-active colloidal clusters. (Reprinted with permission from ref 119. Copyright 1998 IOP Publishing Ltd.)

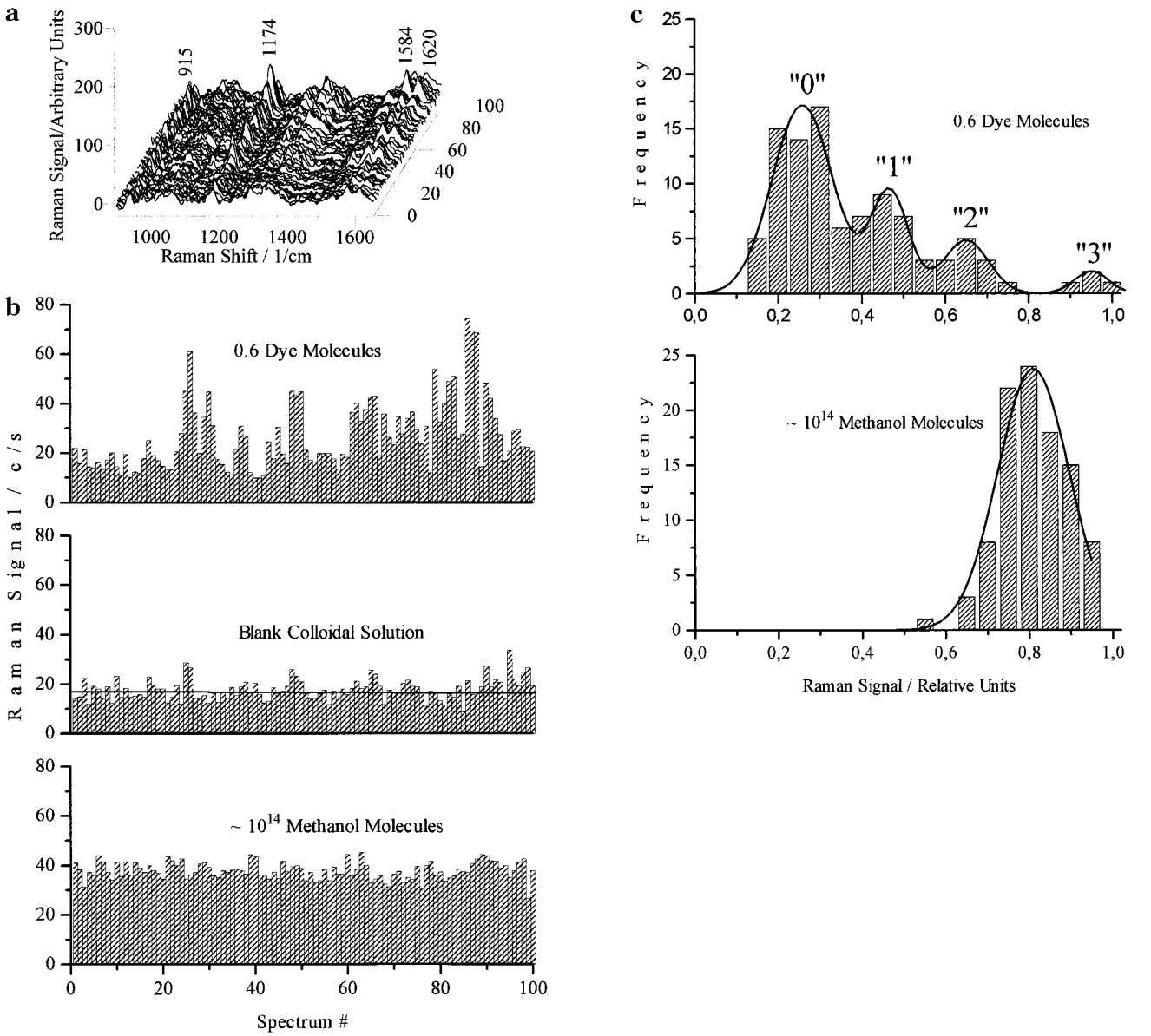

Figure 12. (a) One hundred SERS spectra collected from a 30 pL scattering volume containing an average of 0.6 crystal violet molecules, displayed in the time sequence of measurement. Each spectrum is acquired in 1 s; the laser power was about 150 mW focused to ~12 μm. (b) Peak heights of the 1174 cm^{-1} line for the 100 SERS spectra shown in part a (top). Signals measured at 1174 cm^{-1} from a sample without crystal violet (middle); peak heights of the 1030 cm^{-1} Raman line measured from 3 M (~10^{14} molecules in 30 pL) methanol in silver colloidal solution (bottom). The single-molecule events in the top trace appear at about 38 counts/s, which corresponds to the signal level of ~10^{14} methanol molecules in the bottom trace. (c) Statistical analysis of 100 SERS measurements for an average of 0.6 crystal violet molecules in the probed volume using 20 bins whose widths are 5% of the maximum of the observed signals (x axis). The y axis displays the frequency of the appearance of the appropriate signal levels of the bin. The four peaks reflect the probability of finding just 0, 1, 2, or 3 molecules in the scattering volume (top). Statistical analysis of 100 "normal" Raman measurements at 1030 cm^{-1} of 10^{14} methanol molecules. The solid line is a Gaussian fit to the data (bottom). (Reprinted with permission from ref 32. Copyright 1997 American Institute of Physics.)

are adsorbed on silver colloidal clusters. Analyte concentrations on the order of 10^{-12}—10^{-14} M and probed volumes whose sizes are on the order of femtoliter to picoliter result in average numbers of one or fewer target molecules in the focus volume.

Brownian motion of single-analyte molecule-loaded silver clusters in to and out of the probed volume results in strong statistical changes in the height of Raman signals measured from such a sample in time sequence. This is demonstrated in Figure 12a which shows typical unprocessed SERS spectra measured in time sequence from a sample with an average of 0.6 crystal violet molecules in the probed 30 pL volume. Figure 12b displays the peak heights of the 1174 cm^{-1} line for the 100 SERS spectra, the background level of the colloidal solution with no analyte present, and 100 measurements of the 1030 cm^{-1} Raman line of 3 M methanol in colloidal silver solution (about 10^{14} molecules of methanol in the scattering volume). The normal Raman signal of the 10^{14} methanol molecules appears at the same level as the SERS signal of a single-crystal violet molecule, confirming an enhancement factor on the order of 10^{14}. As expected, the methanol Raman signals collected in time sequence displays a Gaussian distribution (Figure 12c, bottom). In contrast, the

statistical distribution of the 0.6 molecules SERS signal exhibits four relative maxima which are reasonably fit by the superposition of four Gaussian curves. The gradation of the areas of the four statistical peaks are roughly consistent with a Poisson distribution for an average number of 0.5 molecules. This reflects the probability to find 0, 1, 2, or 3 molecules in the scattering volume during the actual measurement. Comparing the measured Poisson distribution, which is in approximate agreement an average of 0.5, with the 0.6 molecule concentration/volume estimate, we conclude that about 80% of the molecules are detected by SERS. The change in the statistical distribution of the Raman signal from Gaussian to Poisson when the average number of target molecules in the scattering volume is one or fewer is evidence for single-molecule detection by SERS. The relatively well "quantized" signals for 1, 2, or 3 molecules suggest relatively uniform enhancement despite the nonuniform shape and size (ca. 10−50 nm) of the silver particles forming the clusters. This might be explained by the "cluster-based enhancement", which has been found to be independent of the individual particle in the cluster and also of the size of the cluster after exceeding a critical cluster size.[52,53,78] To generate a relatively "good" statistical distribution in Figure 12, we choose relatively large probed volumes to generate a balance between the dwell time of the analyte molecule in the probed volume and collection time of the spectra which allows the direct measurement of relatively well-separated 0, 1, and 2 molecule events in the Poisson statistical distribution.

In the resonant single-molecule SERS experiments,[33,86,87] Stokes-shifted signals were recorded from single silver nanoparticles that were spread and immobilized on a polylysine-coated glass surface.[121] Figure 7 shows typical hot nanoparticles used in Nie's and Emory's experiments. Rhodamine 6G was the target molecule, and 514 nm excitation was applied for excitation. As in single-molecule experiments in colloidal solutions, the number of colloidal particles far exceeds the number of analyte molecules. Assuming a random Poisson distribution, the probability of finding more than one molecule on a single particle is extremely small. Thus, the surface-enhanced Raman signals observed from a single nanoparticle should correspond to a single analyte molecule. Evidence for Raman detection of single molecules comes from the strongly polarized nature of the emitted Raman signals and from the observation of sudden spectral and/or intensity fluctuations in the Raman signal. Figure 13 displays surface-enhanced resonance Raman spectra of a single rhodamine 6G molecule collected at 1-s intervals. The Raman signals abruptly change in both frequency and intensity. In general, fluctuations in a spectroscopic signal of a single emitter may be due to changes or fluctuations in the local environment. Nie and Emory suggested that fluctuations in their SERS experiments arise from thermally activated diffusion (site to site hopping) of single adsorbed molecules on the particle surface.

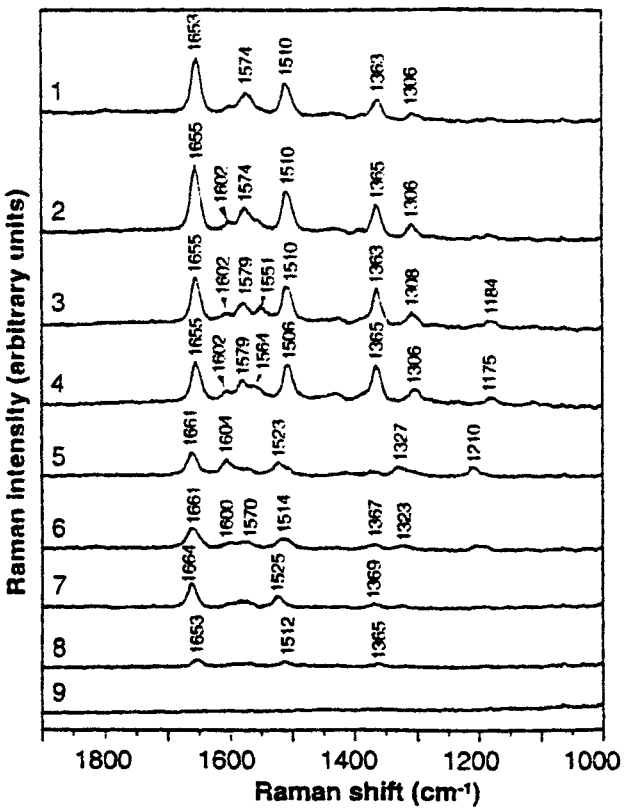

Figure 13. Time-resolved surface-enhanced resonance Raman spectra of a single rhodamine 6G molecule recorded in 1-s intervals. Spectra were excited using 10 μW at 514.5 nm resonant laser radiation focused onto a 500 nm spot size. (Reprinted with permission from ref 33. Copyright 1997 American Association for the Advancement of Science.)

SERRS spectra of single hemoglobin molecules on silver nanoparticles has been reported in ref 86. Figure 14 shows the SERS spectrum of a single hemoglobin molecule. The experimental procedures were similar to those of ref 33. A silver hydrosol of colloidal particles of concentration ~35 pM was prepared by a citrate reduction protocol based on ref 109. The sol was incubated together with a 10 pM solution of human adult met-Hb in order to obtain an average of 0.3 Hb molecules per Ag particle. Dispersed Hb/Ag aggregates were immobilized on polymerized glass or Si surfaces and studied using confocal Raman spectroscopy. Single-molecule SERS spectra were observed from molecules on colloidal dimers (see inset of Figure 14). Due to the near-resonance condition at 514.5 nm excitation, the Hb spectra were dominated by the heme subgroups and were similar to previous SERS and resonance Raman scattering (RRS) studies.[122]

SERRS spectra of individual rhodamine 6G molecules on immobilized silver particles were also studied by exploiting extremely large surface-enhanced resonance Raman cross sections on the order of 10^{-14} cm^2.[87] In contrast to the single-molecule experiments in ref 33, Brus and co-workers observed SERRS from a single rhodamine 6G molecule on small 100−200 nm silver particles created by aggregation of a few colloidal particles. In refs 86 and 87, single-molecule sensitivity was observed on small colloidal aggregates, at least on colloidal dimers.

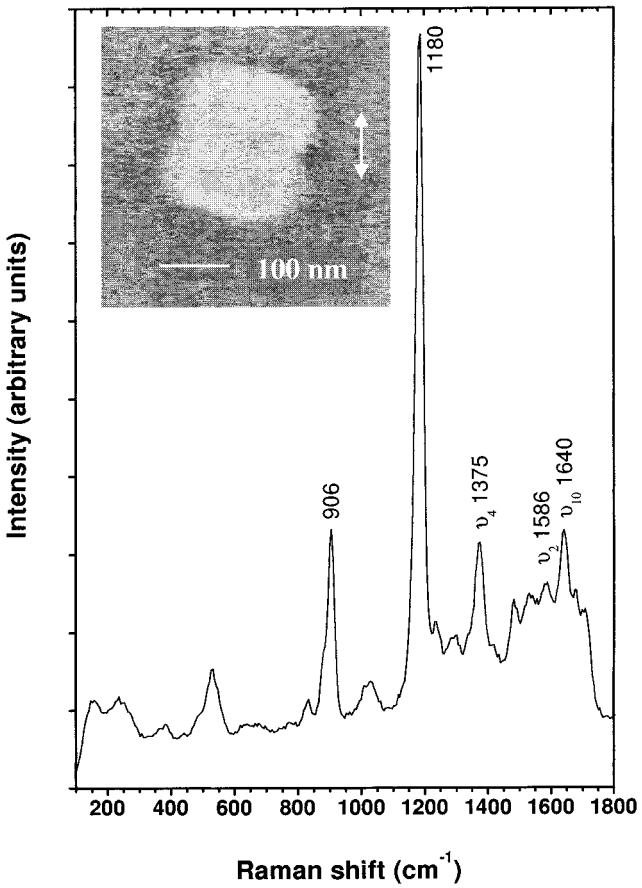

Figure 14. SERS spectrum of a single Hemoglobin molecule on an optically "hot" silver nanoparticle (see inset). A 100× microscope objective was used to illuminate this pair and also to collect the scattered light. The laser wavelength was 514.5 nm, laser power was ~20 μW, laser focus radius was ~1 μm, and integration time was 200 s. (Reprinted with permission from ref 86.)

In all resonant single-molecule experiments, the authors also observed intensity fluctuations including on/off behavior of the SERS signal. Intensity fluctuations or "blinking" has also been reported for fluorescence signals emitted from single molecules[123−125] and single quantum dots.[126]

3.3. Potential of Single-Molecule Raman Detection in DNA Sequencing

One of the most interesting applications for single-molecule detection is in rapid DNA sequencing where one could use spectroscopic detection for identification of single nucleotides. To detect and identify single DNA bases by fluorescence, they must be labeled by fluorescent dye molecules to achieve large enough fluorescence quantum yields and distinguishable spectral properties.[22,34] NIR−SERS provides a method for detecting and identifying a single DNA base which does not require any labeling because it is based on the intrinsic surface-enhanced Raman scattering of the base. Effective Raman cross sections of the order of 10^{-16} cm^2/molecule can be inferred from the observed anti-Stokes to Stokes signal ratios from adenosine monophosphate (AMP) and from adenine on colloidal silver clusters. A comparison between anti-Stokes and Stokes spectra measured from clusters of various sizes confirms SERS enhancement factors independent of cluster size.[52] SERS spectra of adenine and adenosine monophosphate (AMP) are identical, indicating sugar and phosphate bonds do not interfere with the strong SERS effect of adenine.

Samples for single-molecule detection were prepared and checked as described before. The concentrations of small colloidal clusters and adenine were 2×10^{-10} and 3×10^{-11} M, respectively, resulting in clusters containing zero- or one-adenine molecules. Figure 15a represents selected typical spectra collected in 1 s from samples which contain an average of 1.8 adenine molecules in a probed 100-fL volume. Brownian motion of single adenine molecule-loaded silver clusters in to and out of the probed volume results in strong statistical changes in SERS signals measured from such a sample as a function of time. These fluctuations disappear for adenine concentrations 10 times or higher as the number of molecules in the probed volume remains statistically constant. Figure 15b gives the statistical analysis of adenine SERS signals (100 measurements) from an average of 1.8 molecules in the probed volume (top) and from about 18 molecules (below). The change in the statistical distribution of the Raman signal from Gaussian (below) to Poisson (top) reflects the probability to find 0, 1, 2, or 3 molecules in the scattering volume during the actual measurement. Comparing the 1.3 molecule fit with the estimated 1.8 molecule based on concentration/volume, we conclude that 70−75% of the adenine molecules were detected by SERS.

Due to the electromagnetic origin of the enhancement, it should be possible to achieve SERS cross sections for other bases the same order of magnitude as that for adenine when they are attached to colloidal silver or gold clusters. The nucleotide bases show well-distinguished surface-enhanced Raman spectra.[96,127] Thus, after cleaving single native nucleotides from a DNA or RNA strand into a medium containing colloidal silver clusters (for instance, into a flowing stream of colloidal solution or onto a moving surface with silver or gold cluster structure), direct detection and identification of single native nucleotides should be possible due to unique SERS spectra of their bases.

4. Critical Analysis and Prospects of Single-Molecule Raman Spectroscopy

Ultrasensitive Raman spectroscopy at the single-molecule level is based on effective Raman cross sections of the order of 10^{-16} cm^2/molecule which can be achieved by exploiting different effects for enhancing the Raman effect. There is compelling evidence that single-molecule Raman scattering has been observed; however, all experimental observations are not yet fully understood and further investigations are needed for better understanding.

The most obvious rationale for single-molecule detection Raman spectroscopy comes from experimental conditions (low concentrations and small probed volumes/areas), which ensure that only one target molecule can be probed at one time (on average).

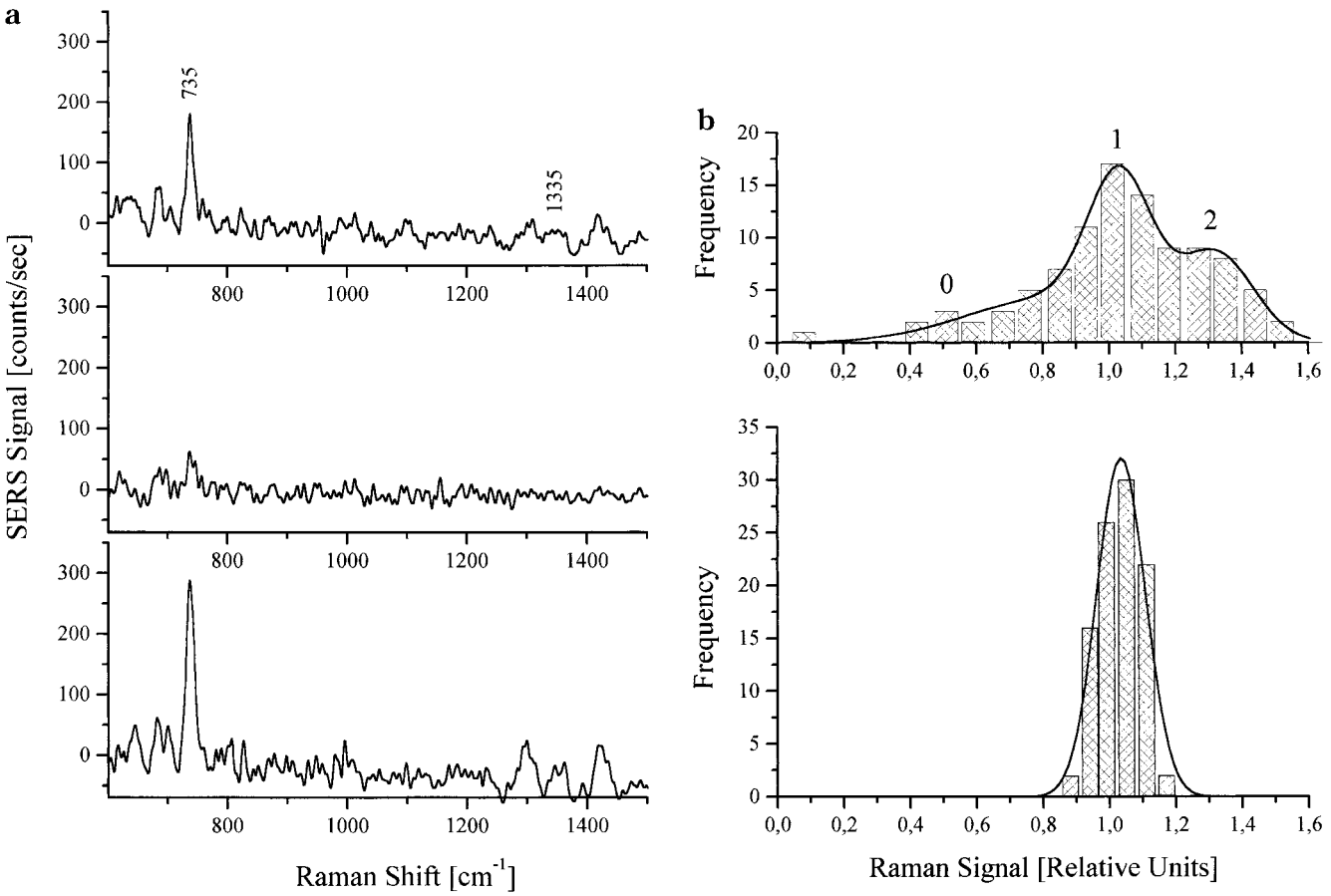

Figure 15. (a) Typical SERS Stokes spectra representing approximately "1" (top), "0" (middle), or "2" (below) adenine molecules in the probed volume (collection time 1 s, 80 mW NIR excitation). (b) Statistical analysis (see Figure 12c) of 100 SERS measurements at an average of 1.8 adenine molecules (top) and for 18 adenine molecules (below) in the probed volume. The experimental data of the 1.8 molecule sample were fit by the sum of three Gaussian curves (solid line) whose areas are roughly consistent with a Poisson distribution for an average number of 1.3 molecules. As expected, the data of the 18 molecules sample could be fit by one Gaussian curve. (Reprinted with permission from ref 52. Copyright 1998 American Institute of Physics.)

Evidence for probing single molecules is different in different SER(R)S studies. In nonresonant near-infrared experiments, single molecules are attached to colloidal clusters in solution, where Brownian motion moves these clusters in to and out of the probed volume. Evidence for single-molecule Raman signals comes from the change in the statistical distribution of the Raman signal from Gaussian to Poisson nature, when the average number of analyte molecules in the probed volume is either one or fewer at best (see Figures 12 and 15).

For the surface-enhanced resonance Raman studies, which were performed on fixed single silver particles, evidence for single-molecule spectra comes from the strongly polarized nature of the emitted Raman signals (which was not observed in population-averaged SERS)[33] and from the observation of sudden spectral fluctuations[33,86,87] (see also Figure 13). However, recent observations of sudden fluctuations or "blinking" in SERRS intensity for higher concentrations of the target molecules[87] appear to be the property of a single metal nanocrystal serving as the SERS-active substrate and may not be related to the observation of a single molecule.

In the near-infrared experiments, nonresonant SERS enhancement factors on the order of 10^{14} are clearly related to the formation of silver or gold colloidal cluster.[31,32,52,53,77] Isolated small spherical silver or gold particles generated enhancement factors of about 10^6 and 10^3, respectively, in agreement with "classical" electromagnetic theories (see section 2). Very large field enhancement, as predicted for colloidal clusters by Shalaev, Moskovits, and coworkers, provides a rationale for single-molecule SERS experiments on colloidal clusters at NIR excitation.[59,62,78] The same enhancement factor obtained independent of cluster size[52] can explain well-quantized SERS signals for 1, 2, and 3 molecules.[32,52,77] This was observed despite the nonuniform sizes and shapes of the SERS-active clusters and also of the individual particles forming the clusters (see section 2).

The formation of colloidal clusters can be increased by adding NaCl to the colloidal solution. Analyte-induced aggregation of the colloidal particles will not play a role for the extremely low analyte concentrations used in single-molecule experiments, where the number of analyte molecules is always smaller than the number of metal particles. The experiments performed with the addition of salt cannot clearly distinguish whether the salt only favors formation of clusters or whether the ions also provide so-called

"active sites" as the prerequisite for a chemical SERS enhancement.

In general, the electromagnetic field enhancement predicted for fractal cluster structures can account for the observed enhancement factors; however, at first glance, field enhancement cannot explain the strong molecular selectivity of the effect. Therefore, one has to think of "electronic" or "chemical" enhancement that might be responsible for the molecular selectivity. On the other hand, actual models of such "electronic" enhancement mechanisms have shown very low enhancement factors compared to electromagnetic field enhancement. Therefore, the absence of "electronic" enhancement does not imply that a measurable SER(R)S effect cannot exist.

Another explanation for the strong molecular selectivity might be related to the high spatial confinement of field enhancement,[55,56,62] which requires that the molecule must be adsorbed on unique small areas of strong-field enhancement. This may not be achieved for all molecules.

Some evidence for a greater role of chemical enhancement in single-molecule SERRS comes from recent experiments performed by Brus and co-workers.[87] They observed extremely large effective SERRS cross sections on the order of 10^{-14} cm^2 for rhodamine 6G on small silver colloidal aggregates, but they did not find a correlation between the intensity of the Rayleigh spectra and the intensity of the SERRS spectra. The strong SERRS signal is not consistent with the model of electromagnetic field enhancement for small compact silver particles. Therefore, the authors's explanation in terms of a model of "electronic" enhancement is in agreement with the ideas suggested by Otto and co-workers.[28,39,40] The huge SERS intensities result from single chemisorbed molecules interacting with ballistic electrons in optically excited large silver particles.[87]

Nie and Emory obtained extremely strong enhancement also for isolated colloidal silver particles.[33] In refs 86 and 87 small aggregates which give rise to some higher field enhancement between the particles[46,86] have been found to be a prerequisite for single-molecule sensitivity. The single-molecule experiments on isolated silver particles cannot benefit from such an additional field enhancement, and explaining such extreme enhancement factors for an isolated colloidal particle is a challenge for theoretical physicists. Polubotko obtained estimates of very strong SERS enhancements by taking into account quadrupole interaction between a strongly increased optical field available in the very close vicinity of unique silver particles with irregular shape, such as rods, and the target molecule.[128]

In general, SERS provides effective cross sections comparable to or even better than fluorescence, thus opening up exciting opportunities for chemical analysis and for Raman spectroscopy in general. The technique is capable of providing rich molecular information for establishing the molecular identity at the single-molecule level. For experiments performed at room temperature and in solutions, SERS is superior to broad and nonspecific fluorescence spectra obtained under similar conditions. Furthermore, nonfluorescent molecules such as nucleotides and amino acids might be detected and identified at the single-molecule level without fluorescence labeling. Quantification of small amounts of substances can be done by counting the number of molecules.

Cross sections of $\sim 10^{-16}$ cm^2/molecule found from vibrational pumping experiments describe conversion into Stokes photons derived from one Raman vibration. The total cross section for generating Stokes light over a frequency range comparable to fluorescence (typically covered by 5−10 Raman lines) will be on the order of 10^{-15} cm^2/molecule, which is about 1 order of magnitude higher than the best known effective fluorescence cross sections. This total cross section for generating Stokes-shifted light is an interesting parameter if one wishes to detect a known molecule without identifying its structure.

It should be noted that near-infrared SERS experiments are nonresonant to the electronic states of the analyte molecule and only vibrational energy is stored in the molecule. Therefore, photodecomposition of the probed molecule should be avoided at higher excitation intensities leading up to saturation.

The maximum number of photons emitted by a molecule in fluorescence or Raman processes under saturation conditions is inversely proportional to the lifetime of the excited states involved in the optical process. Due to the shorter vibrational relaxation times compared to electronic relaxation times, a molecule can go through more Raman cycles than fluorescence cycles per time interval.[113] Therefore, the number of Raman photons per unit time which can be emitted by a molecule under saturation conditions can be higher than the number of fluorescence photons by a factor of 10^2-10^3. This allows shorter integration times for detecting a molecule or higher counting rates for single molecules. Of course, due to shorter vibrational lifetimes, the saturation intensity for a SERS process will be higher than that for fluorescence.

Near-infrared excitation has additional practical spectroscopic applications. The fluorescence background which interferes with single-molecule Raman detection is decreased at longer wavelength excitation. One can avoid this background by using anti-Stokes Raman signals which appear at the high-energy side of the excitation laser radiation.[84] Surface-enhanced anti-Stokes Raman scattering originates from vibrational levels which are populated by the very strong surface-enhanced Raman process. One photon populates the excited vibrational state; a second photon generates the anti-Stokes scattering. Therefore, the anti-Stokes Raman scattering signal depends quadratically on the excitation laser intensity.[31] The Stokes process starts from the vibrational ground state, and one laser photon generates one Stokes photon. The two-photon process inherently confines the volume probed by surface-enhanced anti-Stokes Raman scattering compared to that probed by one-photon "normal" surface-enhanced Stokes scattering.[129] Similar effects of a confinement of the probed volume are known from two-photon-excited fluorescence detection of single molecules.[130,131]

Another interesting aspect of single-molecule Raman experiments comes from the opportunity to study the properties of a single molecule which are hidden under the inhomogeneous line width or averaged out in an ensemble measurement. In general, information related to the local environment of the molecule is lost in the inhomogeneous broadening. In single-molecule Raman spectra, such information can be retrieved and the Raman spectrum of a single molecule can be also a very sensitive probe of the environment of the molecule.

Measurements under the inhomogeneous line width are of particular interest for large molecules that are slightly different in their properties, such as single-wall carbon nanotubes,[132] which exhibit a large inhomogeneous distribution in vibrational frequencies.

To the best of our knowledge, as of now at least five different molecules have been reported to be detected by Raman scattering as singles.[32,33,52,77,86,87] Several experimental findings suggest that a very strong electromagnetic origin is responsible for the large SERS enhancement. Therefore, effective SERS cross sections for single-molecule detection should be available for a wide range of molecules. However, there are molecules (for instance, methanol) that do not show any SERS enhancement, and it is not clear whether one can overcome this molecular selectivity and whether one can achieve large enough effective Raman cross sections for every molecule one wishes to detect. A better understanding of SERS, in general, including adsorption and diffusion processes of molecules on a surface, is an important prerequisite for further development of SERS as a tool for ultrasensitive trace detection. Of course, strong field enhancement does not rule out and may even support a simultaneous "chemical" enhancement which may be present in the SERS effect. Therefore, the "electronic" interaction between a molecule and the metallic nanoparticle is an important issue that needs to be studied in more detail in the future, including (ultrafast time resolved) studies of the "hot" electrons in the metal dots which may be involved in the Raman process.

Resonant and nonresonant SERS studies showed that only a very small number of the molecules in the sample are involved in the Raman process. Extremely large SERS enhancement seems to be a very "local" effect with high spatial confinement, and the single analyte has to find a special hot area (for strong field enhancement) or/and a hot site (for "electronic" enhancement), respectively. SERS spectra of single molecules that are recorded with lateral resolution of a few tens of nanometers using near-field techniques would essentially contribute to an understanding of the local enhancement effects. Also, from an application point of view, screening of single molecules in extremely small volumes using a combination of scanning near-field microscopy and SERS promises exciting opportunities for future developments of microinstrumentation for detection and identification of single molecules in small volumes on the order of attoliters.

5. Acknowledgments

We thank all of our colleagues who have provided us interesting information and material on their work. We are also grateful to the reviewers and the editors for their useful and stimulating comments and suggestions.

6. References

(1) *Infrared and Raman Spectroscopy: Methods and Applications*; Schrader, B., Ed.; John Wiley & Sons: Chichester, 1995.
(2) Ferraro, J. R. *Introductory Raman Spectroscopy*; Academic Press: New York, 1994.
(3) *The Raman Effect*; Turrell, G., Corset, F. J., Eds.; Academic Press: New York, 1996.
(4) *Analytical Raman Spectroscopy*; Grasselli, J. G., Bulkin, B. J., Eds.; John Wiley & Sons: Chichester, 1991.
(5) Laserna, J. J. *Modern Techniques in Raman Spectroscopy*; John Wiley & Sons: Chichester, 1996.
(6) Bloembergen, N. *Pure Appl. Chem.* **1987**, *59*, 1229−1236.
(7) *Chemical applications of nonlinear Raman spectroscopy*; Harvey, A. B., Ed.; Academic Press: New York, 1981.
(8) Zumbusch, A.; Holtom, G. R.; Xie, X. S. *Phys. Rev. Lett.* **1999**, *82*, 4142.
(9) Asher, S. A.; Munro, C. H.; Chi, Z. *Laser Focus World* **1997**, *33*, 99−109.
(10) McCreery, R. L. In *Modern Techniques in Raman Spectroscopy*; Laserna, J. J., Ed.; John Wiley & Sons: Chichester, 1996.
(11) Puppels, G. J.; Mul, F. F. M. D.; Otto, C.; Greve, J.; Robert-Nicoud, M.; Arndt-Jovin, D. J.; Jovin, T. *Nature* **1990**, *347*, 301−3.
(12) Treado, P. J.; Morris, M. D. *Appl. Spectrosc.* **1990**, *44*, 1−4.
(13) McGlashen, M. L.; Davis, K. L.; Morris, M. D. *Anal. Chem.* **1990**, *62*, 846−49.
(14) Brenan, C. J. H.; Hunter, W. *Appl. Opt.* **1994**, *33*, 7520−28.
(15) Smith, D. A.; Webster, S.; Ayad, M.; Evans, S. D.; Fogherty, D.; Batchelder, D. *Ultramicroscopy* **1995**, *61*, 247.
(16) Paesler, M. A.; Moyer, P. J. *Near-Field Optics*; Wiley: New York, 1995.
(17) Jahncke, C. L.; Hallen, H. D.; Paesler, M. A. *J. Raman Spectrosc.* **1996**, *27*, 579−86.
(18) Walker, G.; Hochstrasser, R. In *Laser Techniques in Chemistry*; Myers, A. B., Rizzo, T. R., Eds.; John Wiley & Sons: Chichester, 1995.
(19) Fisher, L. D.; Belle, G. V. *Biostatistics: A Methodology for the Health Sciences*; John Wiley & Sons: Chichester, 1996.
(20) Henlon, E. B.; Shafer, K.; et al. *Phys. Med. Biol.* **1999**, manuscript in preparation.
(21) Moerner, M. E. *Science* **1994**, *265*, 46−53.
(22) Keller, R.; Ambrose, W. P.; Goodwin, P. M.; Jett, J. H.; Martin, J. C.; Wu, M. *Appl. Spectrosc.* **1996**, *50*, 12A.
(23) Rigler, R.; Widengren, J.; Mets, Ü. In *Fluorescence Spectroscopy*; Wolfbeis, O. S., Ed.; Springer: Berlin, 1992.
(24) Nie, S.; Zare, R. N. *Annu. Rev. Biophys. Biomol. Struct.* **1997**, *26*, 567−596.
(25) Xie, X. S.; Trautman, J. K. *Annu. Rev. Phys. Chem.* **1998**, *49*, 441−480.
(26) Jeanmaire, D. L.; Duyne, R. P. V. *J. Electroanal. Chem.* **1977**, *84*, 1.
(27) Albrecht, M. G.; Creighton, J. A. *J. Am. Chem. Soc.* **1977**, *99*, 5215.
(28) Otto, A. In *Light scattering in solids IV. Electronic scattering, spin effects, SERS and morphic effects*; Cardona, M., Guntherodt, G., Eds.; Springer-Verlag: Berlin, Germany, 1984.
(29) Moskovits, M. *Rev. Mod. Phys.* **1985**, *57*, 783−826.
(30) Garrell, R. L., Pemberton, J. E., Garrell, R. L., Pemberton, J. E., Eds.; VCH Publishers: Deerfield Beach, FL, 1994.
(31) Kneipp, K.; Wang, Y.; Kneipp, H.; Itzkan, I.; Dasari, R. R.; Feld, M. S. *Phys. Rev. Lett.* **1996**, *76*, 2444.
(32) Kneipp, K.; Wang, Y.; Kneipp, H.; Perelman, L. T.; Itzkan, I.; Dasari, R. R.; Feld, M. S. *Phys. Rev. Lett.* **1997**, *78*, 1667.
(33) Nie, S.; Emory, S. R. *Science* **1997**, *275*, 1102−6.
(34) Keller, R.; et al. Los Alamos Annual Report, 1990.
(35) Laserna, J. J. *Anal. Chim. Acta* **1993**, *283*, 607−622.
(36) For an overview on SERS trace analytical studies from the $\sim 10^{-7}$ to 10^{-12} M level or approaching detection limits of about 10^4 molecules, see also ref 35.
(37) Fleischman, M.; Hendra, P. J.; McQuillan, A. J. *Chem. Phys. Lett.* **1974**, *26*, 123.
(38) Seki, H. J. *J. Electron Spectrosc. Relat. Phenom.* **1986**, *39*, 239.
(39) Otto, A.; Mrozek, I.; Grabhorn, H.; Akemann, W. *J. Phys. Chem. Condens. Matter* **1992**, *4*, 1143.
(40) Otto, A. International Conference on Raman Spectroscopy XVI, Kapstadt, South Africa, 1998.
(41) Campion, A. *Chem. Soc. Rev.* **1998**, *4*, 241.

(42) Kerker, M.; Siiman, O.; Bumm, L. A.; Wang, D. S. *Appl. Opt.* **1980**, *19*, 3253−5.
(43) Wang, D. S.; Kerker, M. *Phys. Rev. B* **1981**, *24*, 1777−90.
(44) Moskovits, M. *J. Chem. Phys.* **1978**, *69*, 4159.
(45) Moskovits, M. *Solid State Commun.* **1979**, *32*, 59.
(46) Inoue, M.; Ohtaka, K. *J. Phys. Soc. Jpn.* **1983**, *52*, 3853.
(47) Zeman, E. J.; Schatz, G. C. *J. Phys. Chem.* **1987**, *91*, 634−43.
(48) Garcia-Vidal, F. J.; Pendry, J. B. *Phys. Rev. Lett.* **1996**, *77*, 1163−6.
(49) Xiao, T.; Ye, Q.; Sun, L. *J. Phys. Chem. B* **1997**, *101*, 632−8.
(50) Kerker, M. *Appl. Opt.* **1991**, *30*, 4699.
(51) Weitz, D. A.; Oliveria, M. *Phys. Rev. Lett.* **1984**, *52*, 1433.
(52) Kneipp, K.; Kneipp, H.; Kartha, V. B.; Manoharan, R.; Deinum, G.; Itzkan, I.; Dasari, R. R.; Feld, M. S. *Phys. Rev. E* **1998**, *57*, R6281−84.
(53) Kneipp, K.; Kneipp, H.; Manoharan, R.; Hanlon, E. B.; Itzkan, I.; Dasari, R. R.; Feld, M. S. *Appl. Spectrosc.* **1998**, *52*, 1493−97.
(54) Yamaguchi, Y.; Weldon, M. K.; Morris, M. D. *Appl. Spectrosc.* **1999**, *53*, *127*.
(55) Shalaev, V. M. *Phys. Rep.* **1996**, *272*, 61−137.
(56) Poliakov, E. Y.; Shalaev, V. M.; Markel, V. A.; Botet, R. *Opt. Lett.* **1996**, *21*, 1628−30.
(57) Poliakov, E. Y.; Markel, V. A.; Shalaev, V. M.; Botet, R. *Phys. Rev. B* **1998**, *57*, 14901−13.
(58) Shalaev, V. M.; Sarychev, A. K. *Phys. Rev. B* **1998**, *57*, 13265−13288.
(59) Gadenne, P.; Brouers, E.; Shalaev, V. M.; Sarychev, A. K. *J. Opt. Soc. Am. B* **1998**, *15*, 68−72.
(60) Tsai, D. P.; Kovacs, J.; Wang, Z.; Moskovits, M.; Shalaev, V. M.; Suh, J. S.; Botet, R. *Phys. Rev. Lett.* **1994**, *72*, 4149−52.
(61) Zhang, P.; Haslett, T. L.; Douketis, C.; Moskovits, M. *Phys. Rev. B* **1998**, *57*, 15513−18.
(62) Markel, V. A.; Shalaev, V. M.; Zhang, P.; Huynh, W.; Tay, L.; Haslett, T. L.; Moskovits, M. *Phys. Rev. B* **1999**, *59*, 10903.
(63) Aroca, R.; Loutfy, R. O. *J. Raman Spectrosc.* **1982**, *12*, 262−5.
(64) Weitz, D. A.; Garoff, S.; Gersten, J. I.; Nitzan, A. *J. Chem. Phys.* **1983**, *78*, 5324−38.
(65) Pettinger, B. *Chem. Phys. Lett.* **1984**, *110*, 576−81.
(66) Bacackashvilli, A.; Katz, B.; Priel, Z.; Efrima, S. *J. Phys. Chem.* **1984**, *88*, 6185−90.
(67) Hildebrandt, P.; Stockburger, M. *J. Phys. Chem.* **1984**, *88*, 5935−44.
(68) Kneipp, K.; Fassler, D. *Chem. Phys. Lett.* **1984**, *106*, 498−502.
(69) Uphaus, R. A.; Cotton, T. M.; Mobius, D. *Thin Solid Films* **1985**, *132*, 173−184.
(70) Efrima, S. *J. Phys. Chem.* **1985**, *89*, 2843−9.
(71) Kneipp, K.; Kneipp, H.; Rentsch, M. *J. Mol. Struct.* **1987**, *156*, 3−4.
(72) Pettinger, B.; Krischer, K. *J. Electron Spectrosc. Relat. Phenom.* **1987**, *45*, 133−142.
(73) Kneipp, K.; Wang, Y.; Dasari, R. R.; Feld, M. S. *Appl. Spectrosc.* **1995**, *49*, 780.
(74) For "normal" Raman scattering $\sigma(\nu_m)\tau_1(\nu_m)$ is on the order of 10^{-40} cm^2 s. About a 10^{20} W/cm^2 excitation intensity is required to make the Raman pumping comparable to the thermal population of the first vibrational level.
(75) Kaiser, W.; Maier, J. P.; Selmeier, A. In *Laser Spectroscopy IV*; Walther, H., Rothe, E., Eds.; Springer: Berlin, 1979.
(76) Kneipp, K. Unpublished result, 1999.
(77) Kneipp, K.; Kneipp, H.; Deinum, G.; Itzkan, I.; Dasari, R. R.; Feld, M. S. *Appl. Spectrosc.* **1998**, *52*, 175−78.
(78) Stockman, M. I.; Shalaev, V. M.; Moskovits, M.; Botet, R.; George, T. F. *Phys. Rev. B* **1992**, *46*, 2821.
(79) Ziegler, L. D. *J. Raman Spectrosc.* **1990**, *769*.
(80) Murphy, D. V.; Von Raben, K. U.; Chang, R. K.; Dorain, P. B. *Chem. Phys. Lett.* **1982**, *85*, 43−7.
(81) Golab, J. T.; Sprague, J. R.; Carron, K. T.; Schatz, G. C.; van Duyne, R. P. *J. Chem. Phys.* **1988**, *88*, 7942−51.
(82) Kneipp, K.; Kneipp, H.; Seifert, F. *Chem Phys. Lett.* **1995**, *233*, 519.
(83) Hyper-Raman scattering (HRS) is a nonlinear effect which results in a scattering signal that is Raman-shifted relative to the second harmonic of the excitation frequency. Since HRS has a very low scattering cross section, the effect has not been used in practical spectroscopic applications (for a recent overview about hyper-Raman scattering, see ref 79). Hyper-Raman scattering (HRS) can be enhanced in the vicinity of rough metal surfaces or small colloidal metal particles in an analogous fashion to "normal" surface-enhanced Raman scattering (SERS).[80,81] Strong enhancement factors can overcome the inherently weak nature of hyper-Raman scattering, and surface-enhanced Raman and hyper-Raman spectra can appear at comparable intensity levels.[82]
(84) Kneipp, K.; Kneipp, H.; Itzkan, I.; Dasari, R. R.; Feld, M. S. *Chem. Phys.* **1999**, *247*, 155.
(85) Emory, S. R.; Haskins, W. E.; Nie, S. *J. Am. Chem. Soc.* **1998**, *120*, 8009−8010.
(86) Xu, H.; Bjerneld, E. J.; Kåll, M.; Borjesson, L. The 4th International Workshop on Single Molecule Detection and Ultrasensitive Analysis in the Life Sciences, Berlin, Germany, 1998.
(87) Michaels, A. M.; Nirmal, M.; Brus, L. E. *J. Am. Chem. Soc.* **1999**, in press.
(88) Vo-Dinh, T.; Hiromoto, M. Y. K.; Begun, G. M.; Moody, R. L. *Anal. Chem.* **1984**, *56*, 1667−70.
(89) Ni, F.; Cotton, T. M. *Anal. Chem.* **1986**, *58*, 3159−63.
(90) Sequaris, J. M.; Koglin, E. *Anal. Chem.* **1987**, *59*, 525−27.
(91) Carrabba, M. M.; Edmonds, R. B.; Rauh, R. D. *Anal. Chem.* **1987**, *59*, 2559−63.
(92) Campion, A.; Woodruff, W. H. *Anal. Chem.* **1987**, *59*, 1299A.
(93) Lee, N. S.; Hsieh, Y. Z.; Paisley, R. F.; Morris, M. D. *Anal. Chem.* **1988**, *64*, 442.
(94) Ni, F.; Thomas, L.; Cotton, T. M. *Anal. Chem.* **1989**, *61*, 888−94.
(95) Garrell, R. L. *Anal. Chem.* **1989**, *61*, 401A.
(96) Sheng, R.; Nii, F.; Cotton, T. M. *Anal. Chem.* **1991**, *63*, 437.
(97) Bachackashvilli, A.; Efrima, S.; Katz, B.; Priel, Z. *Chem. Phys. Lett.* **1983**, *94*, 571−5.
(98) Baranov, A. V.; Bobovitch, Y. S. *Opt. Spectrosc.* **1982**, *52*, 385.
(99) Baranov, A. V.; Bobovitch, Y. S. *Sov. Phys. JETP Lett.* **1982**, *35*, 143.
(100) Kneipp, K.; Hinzmann, G.; Fassler, D. *Chem. Phys. Lett.* **1983**, *99*, 5−6.
(101) Kneipp, K. Research Report, University Jena, 1986, unpublished results.
(102) Munro, C. H.; Smith, E.; White, P. C. *Analyst* **1995**, *120*, 993.
(103) Tuschel, D. D.; Pemberton, J. E.; Cook, J. E. *Langmuir* **1986**, *2*, 380.
(104) Van Duyne, R. P.; Hulteen, J. C.; Treichel, D. A. *J. Chem. Phys.* **1993**, *99*, 2101−15.
(105) Sudnik, L. M.; Norrod, K. L.; Rowlen, K. L. *Appl. Spectrosc.* **1996**, *50*, 422−4.
(106) Freeman, R. G.; Grabar, K. C.; Allison, K. J.; Bright, R. M.; Davis, J. A.; Guthrie, A. P.; Hommer, M. B.; Jackson, M. A.; Smith, P. C.; Walter, D. G.; Natan, M. J. *Science* **1995**, *267*, 1629−32.
(107) Taranenko, N.; Alarie, J.-P.; Stokes, D. L.; Vo-Dinh, T. *J. Raman Spectrosc.* **1996**, *27*, 379−84.
(108) Szabo, N. J.; Winefordner, J. D. *Anal. Chem.* **1997**, *69*, 2418−25.
(109) Lee, P. C.; Meisel, D. J. *Phys. Chem.* **1982**, *86*, 3391.
(110) Angebranndt, M. J.; Winefordner, J. D. *Talanta* **1992**, *39*, 569−72.
(111) Enlow, P. D.; Buncick, M.; Warmack, R. J.; Vo-Dinh, T. *Anal. Chem.* **1986**, *58*, 1119−23.
(112) The reproducibility does not depend only on a constant size of the enhancement factor. The recorded SERS signal is also strongly dependent on scattering and absorption of laser and Stokes light in the turbid sample solution,[73] where "turbidity" is mainly determined by the aggregation stage of the colloids.
(113) Kneipp, K. *Exp. Techn. Phys.* **1988**, *36*, 161.
(114) Duyne, R. P. V. Personal communication, 1998.
(115) Haller, K. L. Ph.D. Thesis, Northwestern University, 1988.
(116) Taylor, G. T.; Sharma, S. K.; Mohanan, K. *Appl. Spectrosc.* **1990**, *44*, 635−640.
(117) Rodger, C.; Smith, W. E.; Dent, G.; Edmondson, M. *J. Chem. Soc., Dalton Trans.* **1996**, *1996*, 791−799.
(118) Zeisel, D.; Deckert, V.; Zenobi, R.; Vo-Dinh, T. *Chem. Phys. Lett.* **1998**, *283*, 381−85.
(119) Kneipp, K.; Kneipp, H.; Manoharan, R.; Itzkan, I.; Dasari, R. R.; Feld, M. S. *Bioimaging* **1998**, *6*, 104−110.
(120) The stable aggregation stage of the colloids is checked by the absorption/extinction spectrum of the sample solution, which is a very sensitive indicator for coagulation.
(121) Emory, S. R.; Nie, S. *J. Phys. Chem. B* **1998**, *102*, 493−7.
(122) Spiro, T. G.; Strekas, T. C. *J. Am. Chem. Soc.* **1974**, *96*, 338.
(123) Kulzer, F.; Kummer, S.; Matzke, R.; Bräuchle, C.; Th, B. *Nature* **1997**, *387*, 688.
(124) Lu, H. P.; Xie, X. S. *Nature* **1997**, *385*, 143.
(125) Dickson, R. M.; Cubitt, A. B.; Tsien, R. Y.; Moerner, W. E. *Nature* **1997**, *388*, 355.
(126) Nirmal, M.; Dabbousi, B. O.; Bawendi, M. G.; Macklin, J. J.; Trautman, J. K.; Harris, T. D.; Brus, L. E. *Nature* **1996**, *383*, 802.
(127) Thornton, J.; Force, R. K. *Appl. Spectrosc.* **1991**, *45*, 1522.
(128) Polubotko, A. M. *Pure Appl. Opt.* **1998**, *7*, 99−113.
(129) Kneipp, K.; Kneipp, H.; Itzkan, I.; Dasari, R. R.; Feld, M. S. Unpublished result, 1999.
(130) Denk, W.; Strickler, J. H.; Webb, W. W. *Science* **1990**, *248*, 73.
(131) Mertz, J.; Xu, C.; Webb, W. W. *Opt. Lett.* **1995**, *20*, 2532.
(132) Dresselhaus, M. S.; Dresselhaus, G.; Eklund, P. C. *Science of Fullerenes and Carbon Nanotubes*; Academic: San Diego, 1996.
(133) *Raman Spectroscopy in Gases and Liquids*; Weber, A., Ed.; Springer: Heidelberg, 1979.

CR980133R